Synthesis and structures of 5-Nitro-salicylaldehyde thiosemicarbazonates of Copper(II) : molecular spectroscopy, ESI-mass, antimicrobial activity and cytotoxicity

ARTICLE *in* RSC ADVANCES · JANUARY 2015

Impact Factor: 3.84 · DOI: 10.1039/C4RA15006F

6 AUTHORS, INCLUDING:

Harpreet Kaur
O.P. Jindal Global University
37 PUBLICATIONS **113** CITATIONS
SEE PROFILE

Daljit Singh Arora
Guru Nanak Dev University
77 PUBLICATIONS **1,590** CITATIONS
SEE PROFILE

Jerry P. Jasinski
Keene State College
639 PUBLICATIONS **2,502** CITATIONS
SEE PROFILE

RSC Advances

PAPER

Cite this: *RSC Adv.*, 2015, **5**, 14916

Synthesis and structures of 5-nitro-salicylaldehyde thiosemicarb-azonates of copper(II): molecular spectroscopy, ESI-mass studies, antimicrobial activity and cytotoxicity†

Tarlok S. Lobana,*[a] Shikha Indoria,[a] Harpreet Kaur,[b] Daljit S. Arora,[b] Amanpreet K. Jassal[a] and Jerry P. Jasinski[c]

The basic objective of this investigation is to explore potential metallo-organic antimicrobial agents based on metal–thiosemicarbazonates. This study acquires significance in the light of the antibacterial resistance exhibited by Gram-positive and Gram-negative bacteria which have become a serious global medical problem. The increasing drug resistant bacteria are responsible for various nosocomial infections and among these, methicillin resistant *Staphylococcus aureus* (MRSA) is the most frequent nosocomial pathogen. Likewise, *Candida albicans* (fungi) are found to have developed resistance against a number of antifungal agents. In this context, compounds of copper(II) with salicylaldehyde based thiosemicarbazones {5-R′-2-HO–C_6H_4–C^2(H)=N^3–N^2H–C^1(=S)–N^1HR; R = H, Me, Et, Ph: H_2L^1, H_2L^2, H_2L^3, H_2L^4 respective thio-ligands] using bipyridines/phenanthrolines (L′) as co-ligands are being tested against various microorganisms (bacteria/fungi). For R′ = methoxy, several complexes (five coordinate complexes) were tested recently against Gram positive bacteria such as *Staphylococcus aureus* (MTCC740), methicillin resistant *Staphylococcus aureus* (MRSA), Gram negative bacteria, *Shigella flexneri* (MTCC1457), *Klebsiella pneumoniae* (MTCC109), *P. aeruginosa* (MTCC741) and yeast, *Candida albicans* (MTCC227). These complexes displayed significant growth inhibitory action even with low MIC (minimum inhibitory concenteration). A series of new copper(II) complexes (R′ = nitro, keeping R and co-ligands same) namely, [Cu(κ^3-O,N,S–L)(κ^2-*N*,*N*-L′)] {$(L)^{2-}$ = $(L^1)^{2-}$, L′ = bipy, **1**, phen, **2**; $(L)^{2-}$ = $(L^2)^{2-}$, L′ = bipy, **3**, phen, **4**; $(L)^{2-}$ = $(L^3)^{2-}$, L′ = bipy, **5**, phen, **6**; $(L)^{2-}$ = $(L^4)^{2-}$, L′ = bipy, **7**, phen, **8**} have been isolated and characterized by elemental analysis, infrared and electronic absorption spectroscopy, ESR spectroscopy, fluorescence, and single crystal X-ray crystallography. These copper(II) complexes have been investigated for their antimicrobial activity (antibacterial and antifungal activity), viable cell count studies through time kill assays and cellular toxicity testing using MTT assays against the above mentioned bacteria/fungi. Several complexes have shown bactericidal effects with low cytotoxicity towards living cells (sheep blood used).

Received 21st November 2014
Accepted 20th January 2015

DOI: 10.1039/c4ra15006f

www.rsc.org/advances

Introduction

Coordination chemistry of thiosemicarbazones has been in focus since 1960 (ref. 1) and has been well reviewed by Livingstone,[2] Campbell,[3] Padhye *et al.*,[4–6] Casas *et al.*[7,8] and Lobana *et al.*[9] Due to the availability of various donor atoms in mono-thiosemicarbazones (Scheme 1, Structure I) or bis-thiosemicarbazones (Structure II), their metal complexes are of different nuclearity with different structures,[1–29] and there is

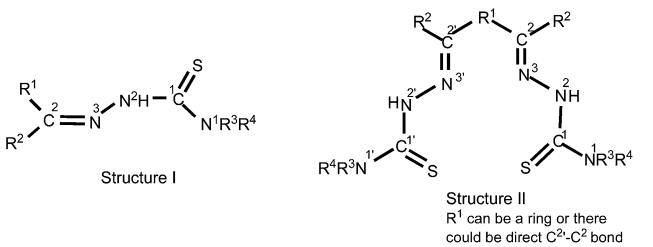

Scheme 1 The types of thiosemicarbazones.

[a]*Department of Chemistry, Guru Nanak Dev University, Amritsar-143 005, India. E-mail: tarlokslobana@yahoo.co.in; Fax: +91-183-2258820*

[b]*Department of Microbiology, Guru Nanak Dev University, Amritsar-143 005, India*

[c]*Department of Chemistry, Keene State College, Keene, NH 03435, USA*

† Electronic supplementary information (ESI) available: The detailed information regarding UV-vis graphs for ligands and complexes, ESI-mass data in detail, Ortep diagrams, Tables 1S and 2S for bond lengths and bond angles is given in ESI. CCDC 1028077, 1028087–1028090, 1028106 and 1028108. For ESI and crystallographic data in CIF or other electronic format see DOI: 10.1039/c4ra15006f

cyclometallation in several cases.[10–12] Thiosemicarbazones/their metal complexes have shown catalytic,[9,13–15] analytical and metal-sensing properties.[9,16–18] The major reason for continued research in the use of thiosemicarbazones lies in their applications, specifically biological ones, either as free ligands[19] or as their metal complexes.[4,9] Owing to our experience in the synthetic coordination chemistry of thiosemicarbazones with various metals (Ni, Pd, Ru Cu, Ag, Au, Hg, Co),[9,20–29] and our recent attempt in investigating the anti-microbial properties of copper(II) complexes,[30] we believed it worthwhile to pursue this area further, the results of which are reported in this paper. However a critical account of the biological applications of metal thiosemicarbazones is briefly reviewed here so as to provide the reader with glimpses of the work being pursued in different laboratories.

The applications of metal derivatives of mono-and bis-thiosemicarbazones with R^1, R^2, R^3, and R^4 at C^2/N^1 groups being other than salicylaldehydic ones are delineated in this paragraph followed by those of metal derivatives of salicylaldehyde based thiosemicarbazones. For example, in one study, $^{64}Cu^{II}$-diacetyl-bis(N^4-methylthiosemicarbazonate) (Structure II) is used for Positron Emisssion Tomography (PET) imaging of hypoxia tissue.[31] Similar complexes have been studied for quantitative structure-relationship models (QSAR) which could be useful for prediction of biological properties such as lipophilicity of complexes.[32] Dilworth *et al.*[33–40] have investigated synthesis of several copper (^{64}Cu)-bis-(thiosemicarbazone) complexes (radiopharmaceuticals) which act as *in vitro* molecular imaging devices and additionally exhibit anticancer activity by inhibition of DNA and RNA synthesis and disruption of ATP production. Interestingly, copper-bis(thiosemicarbazonate) complexes have shown potential neuroprotective activity in cell and animal models of Alzheimer's disease (AD).[41] As regards copper(II) complexes with mono-thiosemicarbazones (Structure I), there is more focus on antimicrobial activities *vis-à-vis* bis-thiosemicarbazone complexes[42–45] in addition to antitumour activities which involve, DNA cleavage, ant-proliferation activity on human leukemic cell lines U937, catalytic inhibition of topoisomerase IIα, cytotoxicity[46–55] and antileishmanial activity.[56]

The bio-chemical status of metal derivatives of salicylaldehyde based thiosemicarbazones was reported recently from our laboratory,[30] wherein it was discussed that complexes reported in literature exhibit antitumor activity,[51,57] photoinduced DNA cleavage[58] and antimicrobial activity.[57–64] It is pointed out here that antimicrobial activity of different types of thiosemicarbazones reported in literature[42–45,51,57–64] has been either exploratory or limited to MIC studies with no attempt to investigate time kill assay and cytotoxicity towards living cells. Further it was observed that there is lack of systematic investigations making it difficult to bring forward the likely useful biological applications which might become possible with intense approach. In this context we have recently reported[30] antimicrobial activity of complexes of copper(II) with salicylaldehyde based thiosemicarbazones as shown in Scheme 2. Complexes showed significant growth inhibitory activity (antimicrobial activity) against methicillin resistant *Staphylococcus aureus* (MRSA), *Staphylococcus aureus*, *Klebsiella pneumoniae*, *Shigella flexneri* and *Candida albicans*. The activity against MRSA is an interesting observation as the commercially available gentamicin is found to be inactive against this bacterial strain.

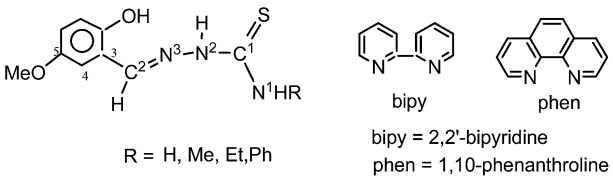

Scheme 2 Thiosemicarbazones and co-ligands.

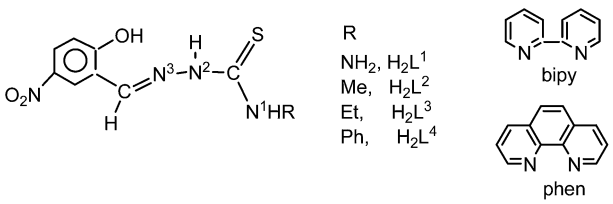

Scheme 3 Thiosemicarbazones and co-ligands.

In this paper, the thio-ligands and co-ligands as shown in Scheme 3 are used for preparing new copper(II) complexes. The 2-hydroxy phenyl ring at C^2 contains nitro group at 5th position as per nomenclature used in this study. Eight new compounds have been characterized using analytical, spectroscopic and structural techniques. Complexes (**1–8**) being reported in this paper have been employed for antibacterial and antifungal activity against Gram positive bacteria such as *Staphylococcus aureus* (MTCC740), methicillin resistant *Staphylococcus aureus* (MRSA), Gram negative bacteria, *Shigella flexneri* (MTCC1457), *Klebsiella pneumoniae* (MTCC109), *P. aeruginosa* (MTCC741) and yeast, *Candida albicans* (MTCC227) respectively. In addition, some of these nitro complexes (with ligands in Scheme 3) as well as some previously reported methoxy compound (with ligands in Scheme 2)[30] are also tested for viable cell count studies through time kill assay and cellular toxicity testing using MTT assay.

Results and discussions

The results of the present investigation are discussed under two main headings: (a) synthesis, structures and spectroscopic properties. This section describes the preparation of new compounds and determination of their molecular structures using X-ray crystallography. In addition the compounds are studied for their spectroscopic properties, fluorescent behavior and ESI mass studies. (b) Complexes as antimicrobial agents and their cytotoxicity. In this section, new compounds isolated have been tested for antibacterial and antifungal activity against *Staphylococcus aureus*, methicillin resistant *Staphylococcus aureus* (MRSA), *Shigella flexneri*, *Klebsiella pneumoniae*, *Pseudamonas aeruginosa* and yeast, *Candida albicans* respectively. In addition, these compounds are also tested for viable cell count studies through time kill assay and cellular toxicity testing using MTT assay.

Synthesis, spectroscopy, ESI mass studies and crystal structures

Reactions of 5-nitro-salicylaldehyde-N-substituted thiosemicarbazones (H_2L) in methanol with copper(II) acetate formed a brown insoluble compound of empirical composition, {Cu(O,N^3,S–L}, which was suspended in dichloromethane–methanol mixture followed by addition of bipyridine/phenanthroline (L′). The resulting dark green solution was allowed to crystallise and thus dark green complexes of stoichiometry, [Cu(O,N^3,S–L)(*N*,*N*-L′)] were obtained (Scheme 4, complexes **1–8**). The complexes are soluble in dichloromethane, methanol, acetonitrile and dimethyl sulfoxide.

Complexes prepared showed IR bands in the region 4000–450 cm^{-1} and a complete set of bands shown by each complex is listed in the Experimental section. The IR spectra of the complexes reveal that the thio-ligands (H_2L^{1-4}) lose –N^2H and –OH hydrogen ions which then coordinate to the metal as dianions (L^{2-}). Further, the diagonistic ν(C=S) bands of the free ligands (1012–1042 cm^{-1}) shift to low energy region, 827–837 cm^{-1} in complexes and these shifts also suggest that the thio-ligands act as anions in complexes. The presence of methanol solvate in complex **1** confirmed by its ν(O–H) band at 3377 cm^{-1}. The ν(N^1–H) bands in complexes **1–8** appear in the range, 3359–3431 cm^{-1}. The electronic absorption spectral data and fluorescence spectral data of complexes **1–8** are listed in the Experimental section. For observing d–d transitions based on Cu^{II} ion, 10^{-3} molar solutions were used and for transitions centered on the ligands and involving charge transfer (CT) bands, the 10^{-4} molar solutions were used (Fig. 1). The electronic spectral bands in the region, 270–286 nm ($\varepsilon = 1.81 \times 10^4$ to 5.00×10^4 L mol^{-1} cm^{-1}) are assigned to $\pi \rightarrow \pi^*$ transitions, 325–335 nm ($\varepsilon = 1.35 \times 10^4$ to 2.63×10^4 L mol^{-1} cm^{-1}) are assigned to $n \rightarrow \pi^*$ transitions. The bands in the region 392–420 nm ($\varepsilon = 1.23 \times 10^4$ to 2.69×10^4 L mol^{-1} cm^{-1}) probably arise due to MLCT electronic absorption bands (Fig. 1a). Complexes have shown absorption in the wide range 500–700 nm (Fig. 1b) with λ^{max} of each complex occurring in the region, 580–600 nm ($\varepsilon = 1.83 \times 10^2$ to 2.8×10^2 L mol^{-1} cm^{-1}). The latter bands appear to occur due to d–d transitions involving energy levels: $^2B_1(d_{x^2-y^2}) \leftarrow {}^2E_g$ (d_{xz}, d_{yz}) which confirmed the divalent oxidation state of Cu.[65] Complexes exhibit fluorescence in the range 368–568 nm with λ_{max} at 426–434 nm corresponding to the excitation wavelength, $\lambda = 320$ nm

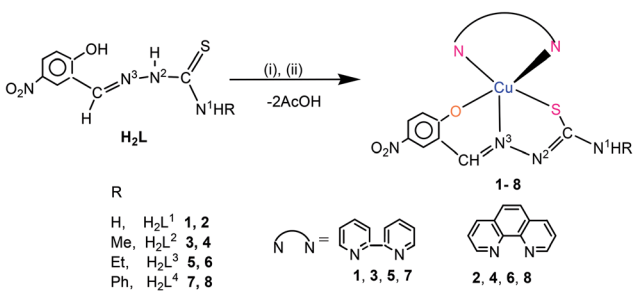

Scheme 4 Synthetic route to complexes **1–8**. (i) $Cu(OAc)_2 \cdot H_2O$; (ii) bipy/phen.

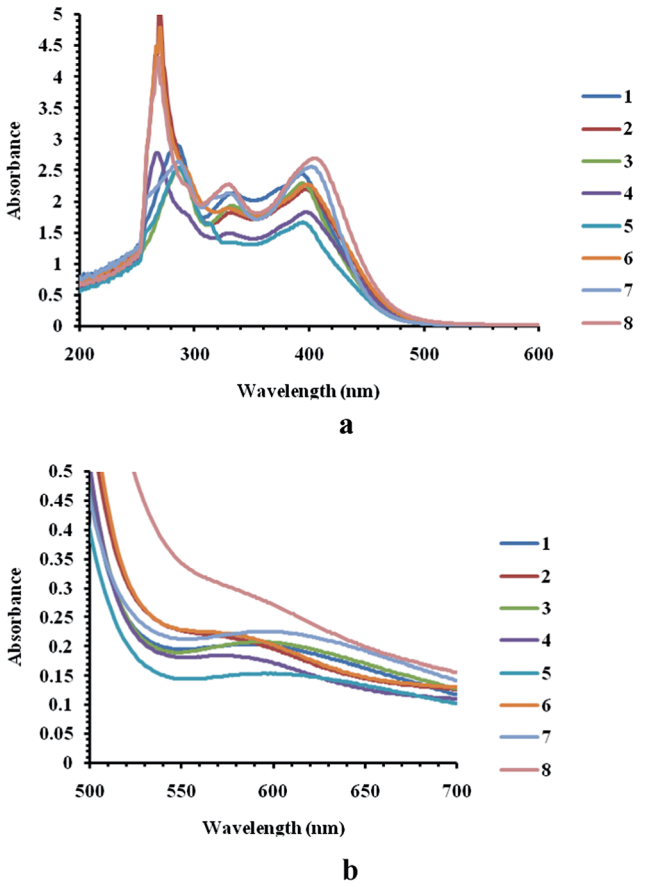

Fig. 1 The electronic absorption spectra of complexes **1–8** (10^{-3}/10^{-4} M).

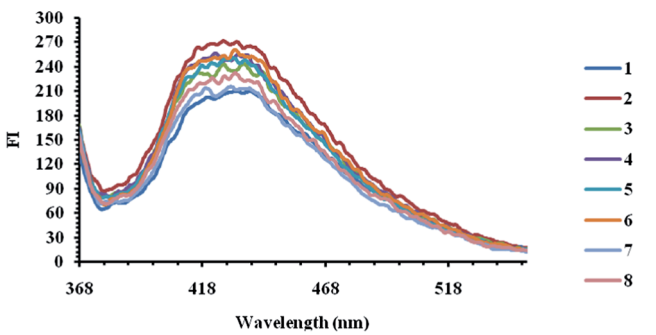

Fig. 2 Fluorescence spectral bands of complexes **1–8**. {λ^{em} = (**1**) 429, (**2**) 426, (**3**) 428, (**4**) 425, (**5**) 430, (**6**) 434, (**7**) 433, (**8**) 426 nm; $\lambda^{ex} = 320$ nm}.

(Fig. 2). The origin of fluorescence appears to be linked to {Cu(*N*,*N*} moiety (*N*,*N* = bipy, phen).

The ESI mass studies of complexes has shown the presence of molecular ions [Cu(O,N,S–L)(*N*,*N*)]$^+$ {L = $(L^{1-4})^{2-}$, *N*,*N* = bipy/phen}, which are listed as follows: [CuL(bipy)+ H]$^+$ (L = L^1 **1**, $C_{18}H_{15}CuN_6O_3S$, *m*/*z* = calcd 458.02, obsd 458.01; L^2 **3**, $C_{19}H_{17}CuN_6O_3S$, *m*/*z* = calcd 472.03, obsd 472.03; L^3 **5**, $C_{20}H_{19}CuN_6O_3S$, *m*/*z* = calcd 486.04, obsd 486.05; L^4 **7**, $C_{24}H_{19}CuN_6O_3S$, *m*/*z* = calcd 534.03, obsd 534.03. [CuL(phen) + H]$^+$ (L = L^1 **2**, $C_{20}H_{15}CuN_6O_3S$, *m*/*z* = calcd 482.03, obsd 482.03;

L^2 **4**, $C_{21}H_{17}CuN_6O_3S$, m/z = calcd 496.04, obsd 496.04; L^4 **6**, $C_{21}H_{19}CuN_6O_3S$, m/z = calcd 510.05, obsd 510.05; L^4 **8**, $C_{26}H_{19}CuN_6O_3S$, m/z = calcd 558.05, obsd 558.05. Fig. 3 shows the molecular ion peak of complex **1** with isotopic pattern (see ESI† for other complexes). Among various complexes, only complex **3** has shown the presence of species, $[Cu(L^2) + H]^+$ ($C_9H_9CuN_3O_3S$, m/z = calcd, 315.97, obsd 315.96) (Fig. 4) with the loss of bipyridine co-ligand. It is interesting to know that ESI-mass studies of complexes **4–6** reveal the formation of dimeric species, $Cu_2(L)_2(N,N)_2]^+$ (L = L^2, *N*,*N* = phen **4**, m/z = calcd 991.07, obsd 991.06; L = L^3, *N*,*N* = bipy **5**, m/z = calcd 971.08, obsd 971.09; L = L^3, *N*,*N* = phen **6**, m/z = calcd 1019.09, obsd 1019.09). Fig. 5 shows the dimeric species of complex **6** along with its isotopic pattern. The dimerisation might have occur through oxygen or sulfur and copper metal center would acquire six coordination in that case. Complexes **1** and **7** have shown another species, namely, $[Cu(bipy)_2 + H]^+$(m/z = calcd 375.06, obsd 375.06) with the loss of thio-ligands (Fig. 6). Similarly, phenanthroline complexes **2**, **4**, **6** and **8** have also shown similar type of species, $[Cu(phen)_2 + H]^+$(m/z = calcd, 423.06, obsd 423.06) (Fig. 7).

Although the complexes have similar stoichiometry, yet molecular structures of complexes **1**, **3–8** except **2** have been obtained. Crystals of complex **1** are orthorhombic with space group $P2_1/c$ while the crystals of **3–8** are triclinic with each having space group $P\bar{1}$ (Table 1). In these complexes, copper is coordinated by phenolato oxygen (O1), azomethine nitrogen (N4), thiolato sulfur (S), and bipy/phen nitrogen atoms, N(1) and N(2). The atoms O, N^3, S (thio-ligand) and one nitrogen of bipy/phen ligand occupy square basal plane while second nitrogen of bipy/phen ligand occupies the axial position. The bond lengths and bond angles of complexes are similar with minor differences as shown in Table 2. In these complexes, the Cu–N_{eq} distances (2.012(4)–2.031(6) Å) are shorter than the Cu–N_{ax} bond distances (2.2400(17)–2.2714(16) Å) related to the co-ligands bipy/phen. Further Cu–$N_{(thio\text{-}ligand)}$ bond distances (1.945(5)–1.965(3) Å) are shorter than the Cu–N_{eq} bond distances as cited above. The trans O–Cu–S bond angles are vary in the range, 150.20(11)–164.56(8)°. The $N_{thio\text{-}ligand}$–Cu–N_{eq} angles are close to 180°. The N_{ax}–Cu–N_{eq} bite angles in the range, 76.1(2)–77.70(9)° are shortest. The τ parameters (the Addison parameters) of complexes vary in the range, 0.132–0.348 which suggest that the molecules are close to square pyramidal geometry. The molecular structures of complexes **1**, **3**, **5**, **7** and **8** are shown in Fig. 8–12 (see ESI† for more details).

The EPR spectra of selected complexes **1–5** and **8** have been obtained (Table 3). Fig. 13–18 show the EPR spectra of complexes. The spectra are partially resolved in parallel and in perpendicular directions (relative the applied field). There is partial resolution of coupling from Cu^{63}(I = 3/2) and thus A_{II}, $A_{\perp}$, g_{II} and $g_{\perp}$ are judiciously calculated. Nevertheless ESR spectra suggest distorted square pyramid geometry in line with the X-ray crystallography.

Complexes as antimicrobial agents and their cytotoxicity

In the context of our objective to develop new metallo-organic antimicrobial agents, a series of new compounds (**1–8**) have been isolated and characterized. These compounds have been tested against Gram negative bacteria, namely, *Klebsiella pneumoniae* 1 (MTCC109), *Shigella flexneri* (MTCC1457), *Pseudomonas aeruginosa* (MTCC741) and Gram positive bacteria, namely, *Staphylococcus aureus* (MTCC740) and methicillin resistant *Staphylococcus aureus* (MRSA). In addition one yeast,

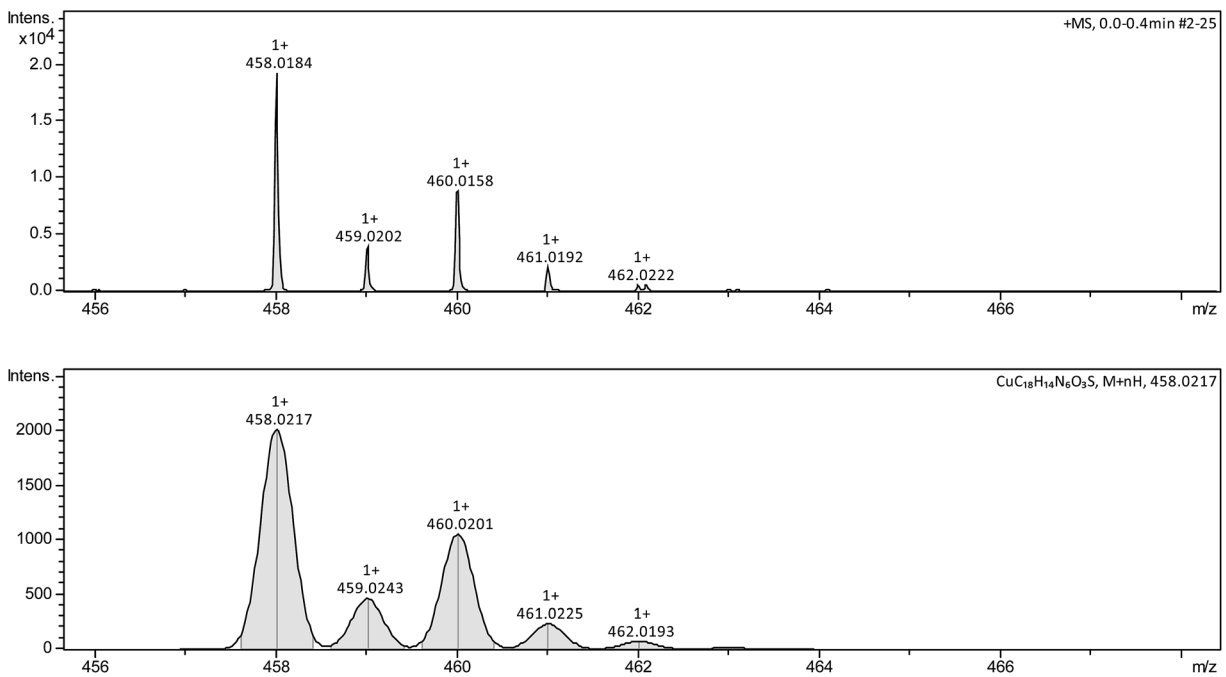

Fig. 3 ESI-mass spectrum due to molecular ion $[CuL^1(bipy) + H]^+$ (m/z = calcd, 458.02, obsd 45.01) with isotopic pattern (complex **1**).

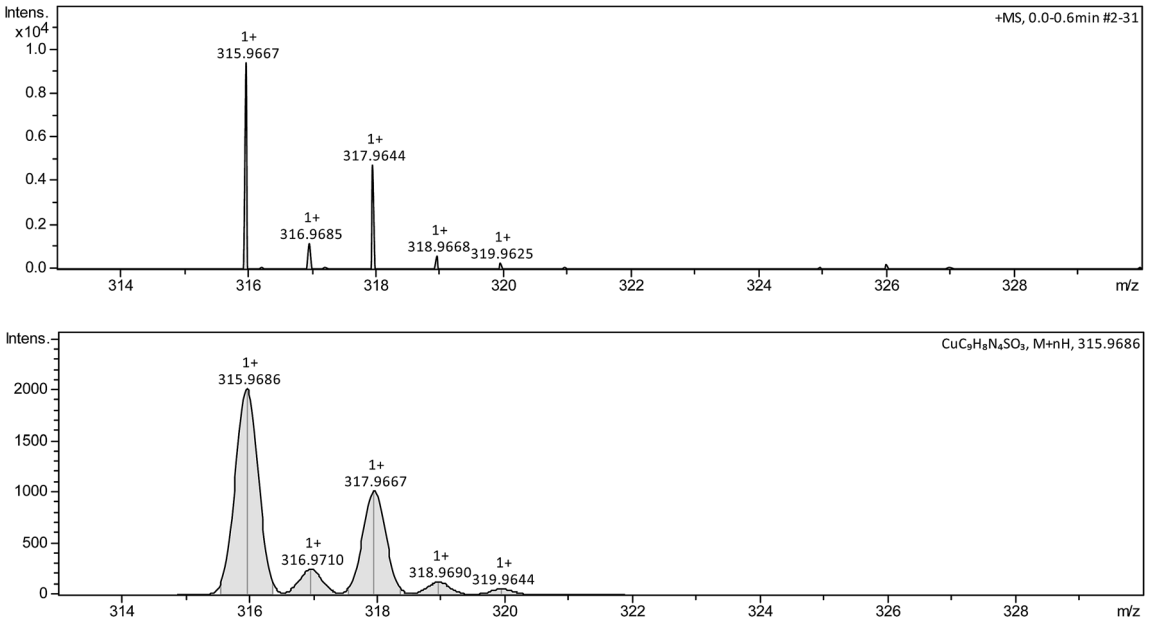

Fig. 4 ESI-mass peak due to $[CuL + H]^+$, (m/z = calcd, 315.97, obsd 315.96) species with isotopic pattern (complex **3**).

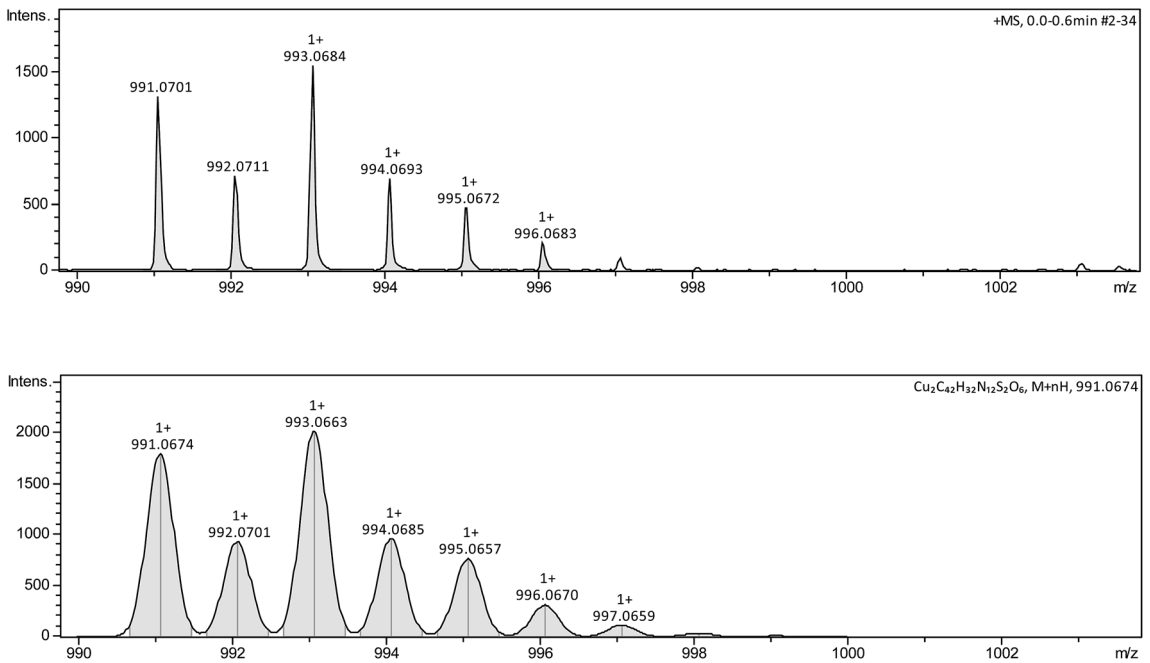

Fig. 5 ESI-mass peak of dimer $[Cu_2(L^2)_2(phen)_2 + H]^+$ (m/z = calcd, 991.07, obsd 991.06) with isotopic pattern (complex **4**).

Candida albicans (MTCC227) has also been studied. This study acquires significance in the light of the antibacterial resistance exhibited by Gram-positive and Gram-negative bacterias which have become a serious global medical problem. The increasing drug resistant bacteria are responsible for various nosocomial infections and among these, methicillin resistant *Staphylococcus aureus* (MRSA) is the most frequent noscomial pathogen.[66,67] In literature, a series of organic based antibacterial agents such as aminoglycoside, dalfopristin, teicoplanin, linezolid, methicillin, gentamicin, kanamycin, neomycin, streptomycin and amikacin have been used/are in use for the treatment of bacterial infections. However, in several cases, there are side effects such as oxotoxicity, dose-related nephrotoxicity *etc.*[68–72] The efficacy of some antibiotics, *e.g.* methicillin, is restricted due to the development of resistant mutants such as methicillin resistant *staphylococcus aureus* (MRSA).[66,67,72] Similarly, a series of anti-fungal agents such as fluconazole and amphotericin have been used for the treatment of *Candida albicans* (fungal pathogen), however, use of these antibiotics causes nozea and hepatotoxicity. Moreover, *Candida albicans*

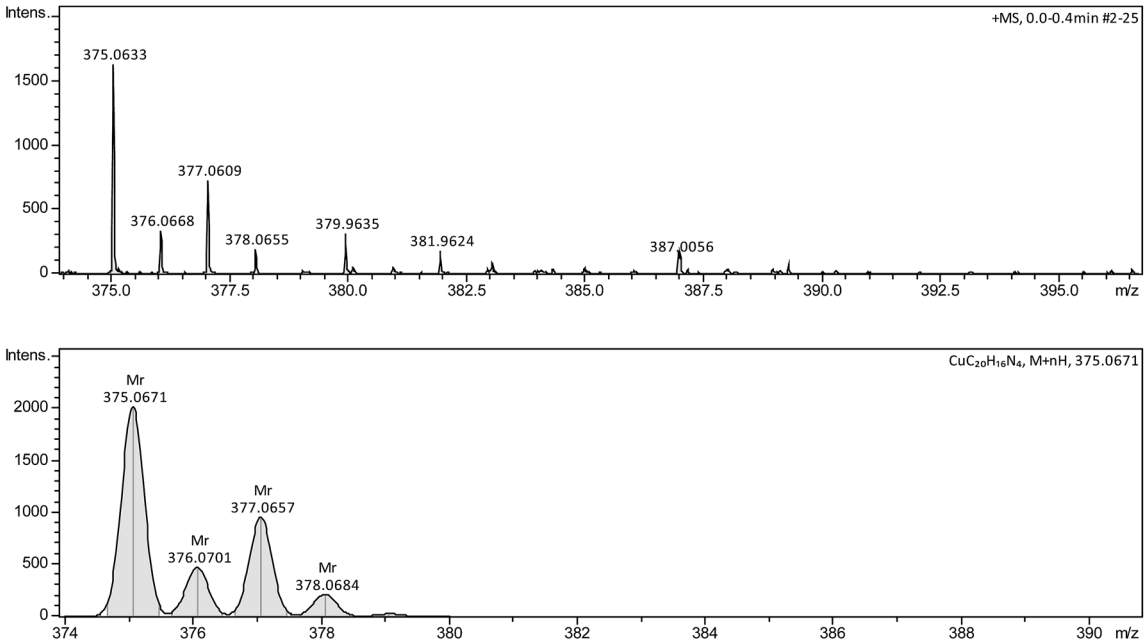

Fig. 6 ESI-mass peak due to $[Cu(bipy)_2 + H]^+$ (m/z = calcd, 376.06, obsd 375.06) species with isotopic pattern (complex **1**).

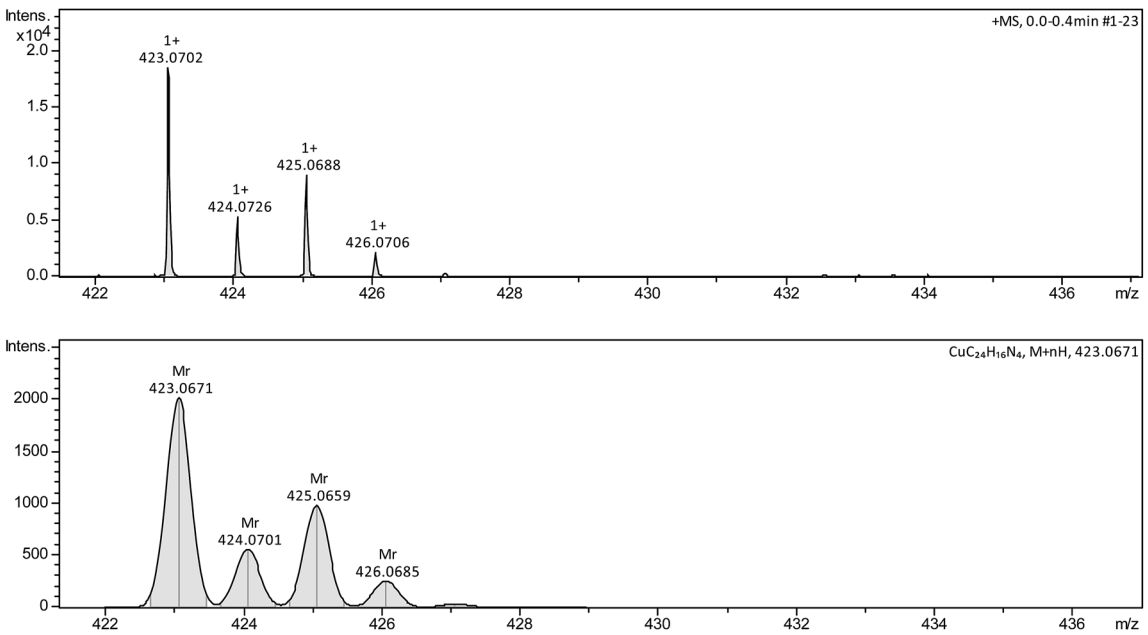

Fig. 7 ESI-mass peak due to $[Cu(phen)_2 + H]^+$(m/z = calcd, 423.06, obsd 423.06) species with isotopic pattern (complex **2**).

are found to have developed resistance against a number of antifungal agents.[72–75]

From above, it may be noted that there is a critical need to develop new antibacterial agents for difficult to treat multidrug resistant bacteri and fungi and thus invited the search for new antimicrobial agents, a challenging task for chemists.[76,77] As highlighted in the introduction, metal–thiosemicarbazone complexes have shown various biological applications such as antitumour activities which involve, DNA cleavage, antproliferation activity on human leukemic cell lines U937, catalytic inhibition of topoisomerase IIα, cytotoxicity,[46–55] antileishmanial activity,[56] antimicrobial activity[51,57–64] and neuroprotective activity in cell and animal models of Alzheimer's disease (AD).[41] It is added here that the antimicrobial activity reported in literature were preliminary in nature.[51,57–64]

Keeping in view, the necessity to explore new antimicrobial agents as highlighted above and also owing to our interest in metal–thiosemicarbazone coordination chemistry, recently,[30] antimicrobial properties of copper(II) with salicylaldehyde-N-substituted thiosemicarbazones with thio-ligands shown in

Table 1 Crystallographic data for complexes **1**, **3–8**

	1	**3**	**5**	**7**	**4**	**6**	**8**
Formula	$4(C_{18}H_{14}CuN_6O_3S)\cdot 3(CH_3OH)$	$C_{19}H_{16}CuN_6O_3S$	$C_{20}H_{18}CuN_6O_3S$, 3(O)	$C_{24}H_{18}CuN_6O_3S$	$C_{21}H_{16}CuN_6O_3S$	$C_{22}H_{18}CuN_6O_3S$	$C_{26}H_{18}CuN_6O_3S$
M	1928.01	472.00	540.05	534.06	496.00	510.02	558.08
T(K)	293(2)	296(2)	296(2)	296(2)	173(2)	173(2)	296(2)
Crystal system	Monoclinic	Triclinic	Triclinic	Triclinic	Triclinic	Triclinic	Triclinic
Space group	$P2_1/c$	$P\bar{1}$	$P\bar{1}$	$P\bar{1}$	$P\bar{1}$	$P\bar{1}$	$P\bar{1}$
a (Å)	16.3302(4)	8.073(2)	8.1557(18)	7.8808(6)	5.9763(5)	7.9073(4)	7.7532(6)
b (Å)	20.2955(5)	9.391(3)	11.023(3)	10.9146(9)	11.6828(10)	11.5507(6)	12.0716(9)
c (Å)	25.5819(7)	13.924(4)	14.092(3)	14.0860(9)	14.3427(8)	14.2629(8)	14.2178(9)
α (°)	90.00	71.441(15)	104.400(13)	99.182(3)	85.970(6)	104.034(5)	103.320(4)
β (°)	107.3830(10)	85.420(15)	93.284(13)	94.515(3)	83.926(6)	104.217(5)	99.041(4)
γ (°)	90.00	75.557(16)	99.663(14)	102.572(3)	82.198(7)	100.871(5)	105.263(4)
V (Å^3)	8091.4(4)	969.1(5)	1203.1(5)	1159.29(15)	984.98(13)	1181.69(12)	1215.14(16)
Z	4	2	2	2	2	2	2
R_1	0.0566	0.0675	0.0787	0.0338	0.0381	0.0505	0.0591
wR_2 (R_{Indices})	0.1733	0.1853	0.2088	0.0911	0.0896	0.1328	0.1087
R_1	0.1005	0.1888	0.1598	0.0450	0.0527	0.0591	0.0417
wR_2 (all data)	0.2377	0.3256	0.2624	0.0986	0.0984	0.1328	0.0993

Table 2 Bond distances (Å) and bond angles (°) in complexes[a]

Bipy complexes [Cu(κ^3-O,N,S–L)(κ^2-*N*,*N*)]					Phen complexes [Cu(κ^3-O,N,S–L) (κ^2-*N*,*N*)]		
	1	**3**	**5**	**7**	**4**	**6**	**8**
Cu–O	1.974(4)	1.942(5)	1.961(3)	1.9515(16)	1.9699(14)	1.940(2)	1.947(2)
Cu–N	1.953(4)	1.944(5)	1.959(4)	1.949(3)	1.9492(15)	1.965(3)	1.951(2)
Cu–S	2.2510(14)	2.253(2)	2.2828(14)	2.2902(6)	2.2694(5)	2.2737(8)	2.2940(8)
Cu–N_{eq}	2.012(4)	2.031(6)	2.031(4)	2.0125(17)	2.0161(15)	2.024(3)	2.009(2)
Cu–N_{ax}	2.250(5)	2.253(6)	2.241(4)	2.2400(17)	2.2714(17)	2.306(3)	2.276(2)
O–Cu–N	92.45(16)	93.6(2)	93.04(16)	92.20(6)	92.96(6)	92.62(10)	92.17(9)
N–Cu–S	86.23(12)	85.26(6)	84.96(12)	85.25(9)	85.34(5)	85.54(8)	87.85(8)
O–Cu–S	150.20(11)	162.04(19)	162.80(13)	160.58(5)	156.03(5)	164.56(8)	161.54(7)
N–Cu–N_{eq}	171.11(18)	175.3(2)	174.95(16)	177.60(7)	174.46(7)	172.46(10)	177.18(10)
N_{eq}–Cu–N_{ax}	77.05(18)	76.1(2)	76.62(15)	77.00(7)	77.67(6)	77.47(10)	77.72(9)
τ value	0.348	0.221	0.204	0.283	0.307	0.132	0.260

[a] ax = axial; eq = equatorial.

Scheme 2 were investigated. All the complexes exhibited significant antimicrobial activity against methicillin resistant *Staphylococcus aureus* (MRSA), *Staphylococcus aureus*, *Klebsiella pneumoniae*, *Shigella flexneri* and *Candida albicans* {using well diffusion method (zone of inhibition) and minimum inhibitory concentration (MIC) studies}. Specifically, complexes **9** and **10** (Scheme 5) have shown most significant antimicrobial activity against various bacteria and fungi. Here in this paper, the eight newly synthesized compounds of copper(II) as shown in Scheme 4 are tested for their antimicrobial activity *via* well diffusion method, MIC studies, time kill study through viable cell count method and Cellular toxicity testing using MTT assay. Complexes **9** and **10** previously reported are also tested for time kill study through viable cell count method and Cellular toxicity testing using MTT assay.

Antimicrobial activity-zone of inhibition

Table 4 shows biological data for antimicrobial activities of copper(II) complexes with salicylaldehyde-N-substituted thiosemicarbazones, [Cu(κ^3-O,N,S–L) (*N*,*N*-donor)] **1–8** (labeled as Class I compounds). For comparison purpose, the data for antimicrobial activities of precursors, $[Cu(\kappa^3\text{-O,N,S–L})]_n$ without bipyridine or phenanthroline bases (Class II compounds) as well as those of thio-ligands under discussion {see Scheme 3, $H_2L = H_2L^1$, H_2L^2, H_2L^3, H_2L^4} (Class III compounds) are also given in Table 4. It is apparent from the data given in Table 4, that the antimicrobial activity varies in the order: Class I > Class II > Class III. Thus the metallo-organic class I compounds **1–8** become the preferred choice for antimicrobial activity and some most significant observations made are presented as follows. It is very interesting to note that all these complexes have shown significant antimicrobial activity against *Klebsiella pneumoniae* (MTCC109), *Shigella flexneri* (MTCC1457), *Pseudomonas aeruginosa* (MTCC741) *Staphylococcus aureus* (MTCC740), methicillin resistant *Staphylococcus aureus* (MRSA) and *Candida albicans* (MTCC227). It may be noted from Table 4, that complexes **5–8** (R substituent at N^1: ethyl **5**, **6**; phenyl **7**, **8**) have shown highest

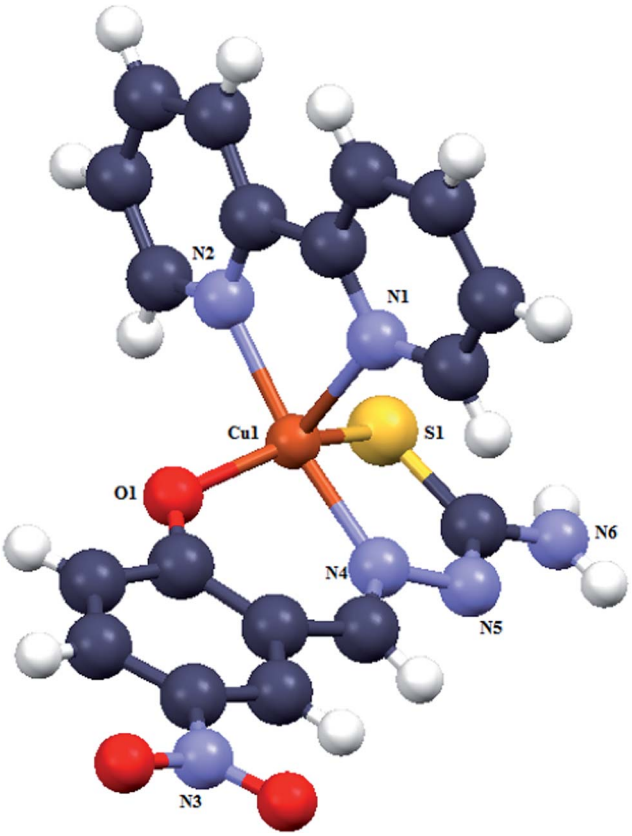

Fig. 8 A view of one of the four independent molecules of complex [Cu(κ^3-O,N,S–L^1) (κ^2-*N*,*N*-bipy)] **1**.

antimicrobial activity ranging from 24–28 mm zone of inhibition (zoi) against methicillin resistant *Staphylococcus aureus* (MRSA). Other complexes **1–4** (R substituent at N^1: hydrogen, **1**, **2**; methyl **3**, **4**) have shown antimicrobial activity around 20 + 1 mm zone of inhibition (zoi) against MRSA. This is an interesting observation as the commercially available Gentamicin is found to be inactive against this bacterial strain. As regards *Staphylococcus aureus*, complexes **5–8** exhibited activity in the range, 23–26 mm zoi which falls in the range of activity shown by Gentamicin (25 mm zoi) (Table 4). The activity of other complexes for this bacterial strain is less (19–20 zoi). Further the activity of **5**, **7** and **8** against *Klebsiella pneumoniae* is highest (25–30 mm zoi) *vis-à-vis* to that of other complexes (20–23 mm zoi). Only complex **7** (30 mm zoi) showed activity close that of Gentamicin (32 mm zoi). It is interesting to note that the complexes have shown activity against *Shigella flexneri* (18–22 mm zoi) and *Pseudomonas aeruginosa* (18–24 mm zoi) either close to or higher than standard antibiotic *i.e.* Gentamicin (17 mm zoi). It may be noted that when R′ = methoxy, the copper(II) complexes were either not active or showed poor activity against these bacterial strains.[30] Complexes **5–8** showed highest activity (31–35 mm zoi) against yeast, *Candida albicans* which is comparable to that of commericial Amphotericin (34 mm zoi) while other complexes showed low activity (24–33 mm zoi).

Minimum inhibitory concentration (MIC)

It can be seen from Table 5 that several complexes were active at minimum inhibitory concentration (MIC) of 10 μg mL^{-1} (methicillin resistant *staphylococcus aureus*: **7**, **8**; *Klebsiella pneumoniae*

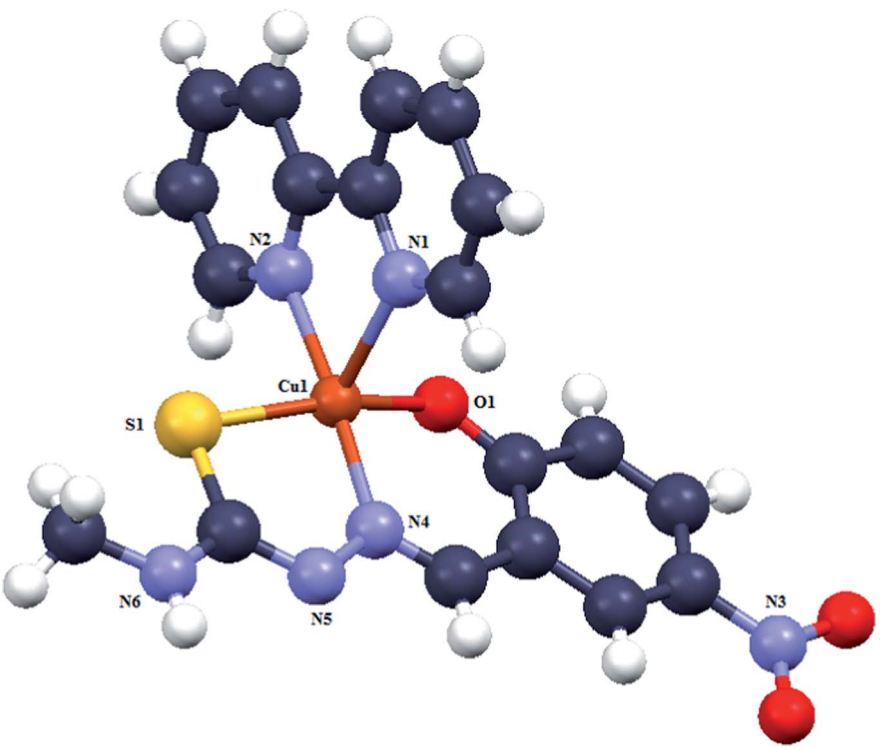

Fig. 9 Molecular structure of complex [Cu(κ^3-O,N,S–L^2)(κ^2-*N*,*N*-bipy)] **3**.

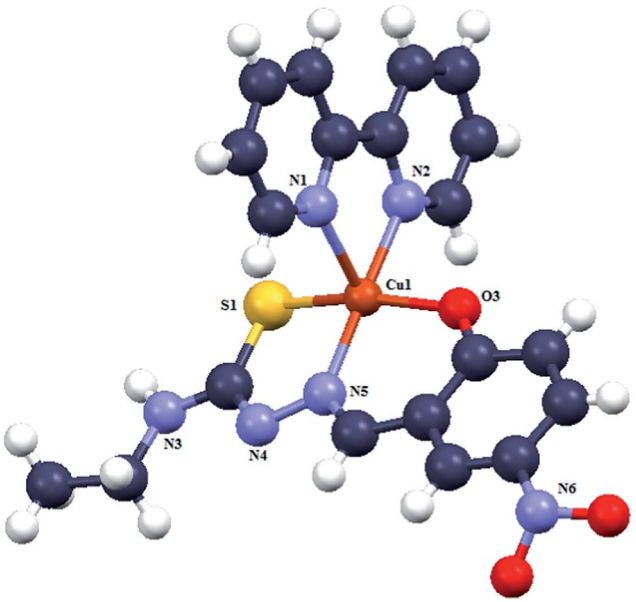

Fig. 10 Molecular structure of complex [Cu(κ^3-O,N,S–L^3) (κ^2-*N*,*N*-bipy)] **5**. Here, water molecules are omitted for simplification of the diagram but these are shown in ortep diagram given in ESI.†

1: **7**, **8**; *Candida albicans*: **6**) and MIC of 50 μg mL^{-1} (methicillin resistant *staphylococcus aureus*: **5**, **6**; *Staphyloccus aureus*: **5–8**; *Klebsiella pneumoniae* 1: **5**, **6**; *Pseudomonas aeruginosa*: **6**, **7**). Further, MIC of 250–750 μg mL^{-1} was required for methicillin resistant *staphylococcus aureus* (**1–4**), *Staphyloccus aureus* (**1–4**), *Klebsiella pneumoniae* (**1–4**), *Shigella flexneri* (**1–8**) and *Pseudomonas aeruginosa*, (**1–5**, **8**). Interestingly, *Candia albicans* was found to be the most sensitive organism with the lowest MIC of 5 μg ml^{-1} for complexes **5**, **7** and **8**. MIC of 10–50 μg mL^{-1} was found against *C. albicans* with complexes, **1–4** and **6**.

Time kill assay

In this investigation, apart from zone of inhibition and MIC studies, some complexes have been tested further for time kill assay by viable cell count studies and cellular toxicity *via* MTT Assay. The complexes selected for the latter studies are the ones which showed high zone of inhibition with lowest MIC. In this context complexes **7** and **8** with phenyl substitution at N^1 (present studies) along with complexes **9** and **10** with phenyl substitution at N^1 (previous studies, see Scheme 5)[30] are used for carrying out time kill assay by viable cell count studies and cellular toxicity *via* MTT Assay. Complexes **1** and **2** with both hydrogen substitutions at N^1 atom are also included in this study for comparison purpose. It is added here that *in vitro* time kill assay determines the rate and extent of antimicrobial activity and provides more accurate description of antimicrobial agents than does the MIC.[78] Time kill studies not only give the information about the nature of the antimicrobial agent whether a particular agent is bactericidal or bacteriostatic but also the time taken by the antimicrobial agent for complete killing of the particular microorganism. It also provides relative indication of the potential *in vivo* activity of the new antimicrobial agents, which can be further useful in various pharmaceutical purposes used in drug development. On the basis of 1× MIC of the compound obtained for different organisms they were subjected to viable cell count studies.

From time kill assay done by viable cell count studies (Fig. 19–21), it is revealed that complex **7** showed 80% killing of MRSA at 0 h of incubation. complex **7**, [Cu(L^4) (bipy)]{R = Ph} killed 80% of MRSA at 0 hour of incubation and the remaining

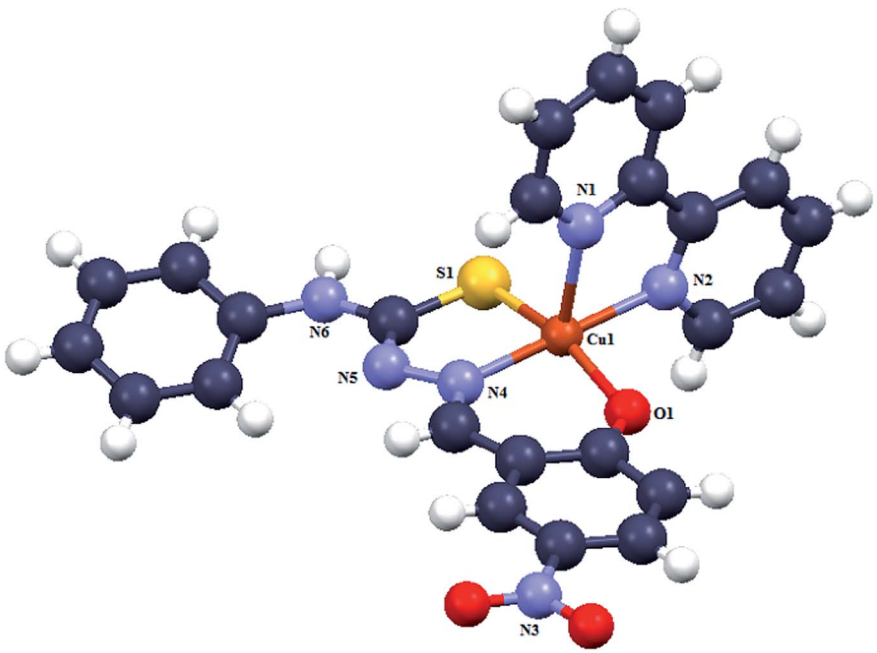

Fig. 11 Molecular structure of complex [Cu(κ^3-O,N,S–L^4)(κ^2-*N*,*N*-bipy)] **7**.

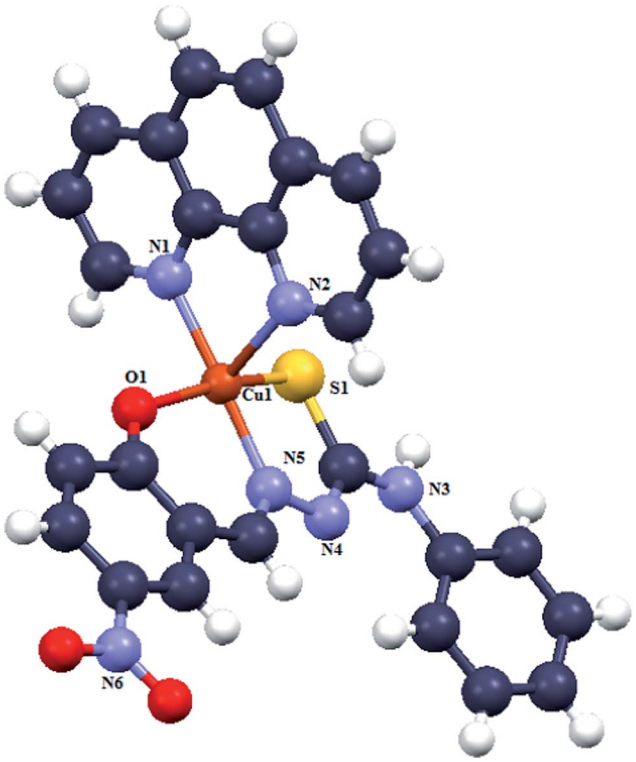

Fig. 12 Molecular structure of complex [Cu(κ^3-O,N,S–L^4)(κ^2-*N*,*N*-phen)] **8**.

20% of viable cells of MRSA were killed in 2 hours of incubation. Complex **8**, [Cu(L^4) (phen)]{R = Ph} showed similar behavior but killing was 70% at 0 hour of incubation and a complete killing of remaining 30% viable cells occurred in 4 hours. Complexes, [Cu(L)(bipy)]{R = Ph} **9** and [Cu(L)(phen)]{R = Ph} **10** with methoxy substitution at 2-hydroxyphenyl ring of thio-ligand (Scheme 5), only 60% of MRSA was killed at 0 hour of incubation and the remaining 40% of viable cells were killed in 4 hours. It is inferred from here that complexes **7** and **8** with nitro substitution at 2-hydroxyphenyl ring of thio-ligand are most effective antibacterial agent against MRSA. It may be noted that complexes **1** and **2** with H_2L^1 ligand (hydrogen substitution at N^1 atom) showed killing effect, similar to complexes **9** and **10**. This demonstrates that the substituent in the 2-hydroxyphenyl ring of thio-ligands also plays important role in determining antimicrobial behavior.

The behavior of complexes **7**–**10** was similar for *S. aureus*. About 30–35% of *S. aureus* was killed at 0 hour of incubation and the remaining 70–65% of viable cells of bacteria was killed in 6–8 hours of incubation. Complexes **1** and **2** killed 40–45% of *S. aureus* bacteria at 0 hour of incubation and remaining 60–65% viable cells were killed in 6-10 hours of incubation. Similarly, 70–80% of *K. pneumoniae* got killed by complexes **7**–**8** at 0 hour of incubation and remaining 20–30% was killed at 2–4 hours of incubation. The other complexes **9**, **10** as well as **1** and **2** showed longer time for complete killing (Fig. 13–15). Further, 40–45% of *Sh. flexneri* was killed by complexes **7** and **8** at 0 hour of incubation and remaining 55–60% viable cells were killed in 8–10 hours of incubation. Interestingly, complexes **9** and **10** killed 35% of bacteria at 0 hour of incubation and remaining 65% of viable cells were killed in 6 hours of incubation. The behavior of complexes **1** and **2** is nearly similar to that of complexes **7** and **8**. For *P. aeruginosa*, complexes **7** and **8** killed only 30% of bacteria at 0 hour of incubation and the remaining

Table 3 EPR data of complexes (**1**–**5**, **8**)

Complex	Parallel region	Perpendicular region	$A_{II(gauss)}$	$A_{\perp(gauss)}$	g_{II}	$g_{\perp}$	g_{iso}
1	3065, 3124	3233.8, 3267, 3308	59	58	2.168	2.052	2.091
2	—	3152, 3236, 3287	—	93	—	2.084	2.084
3	3053	3250, 3278, 3295	—	31	2.198	2.050	2.099
4	3059	3219, 3269, 3310	—	66	2.194	2.055	2.101
5	3060	3242, 3270, 3284	—	28	2.193	2.056	2.102
8	3055	3244, 3264, 3293	—	39	2.196	2.053	2.101

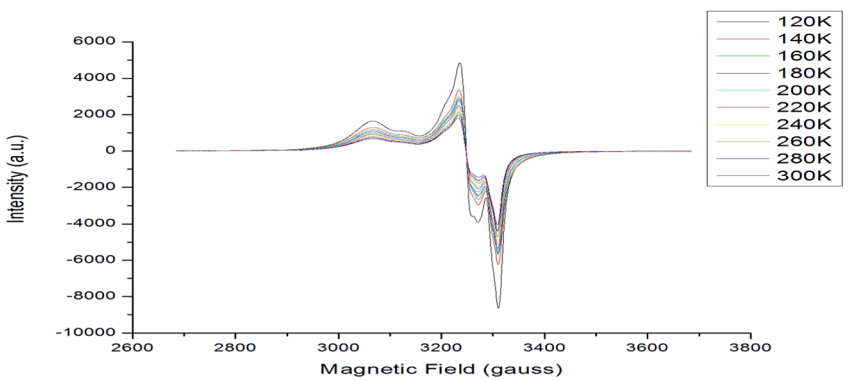

Fig. 13 X-band EPR spectrum of complex **1**.

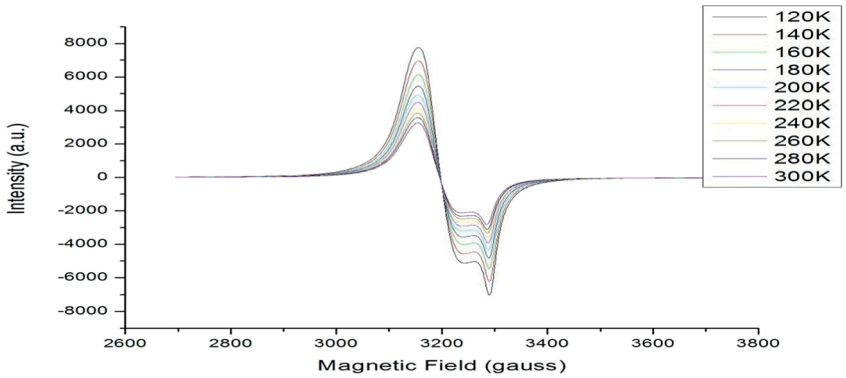

Fig. 14 X-band EPR spectrum of complex **2**.

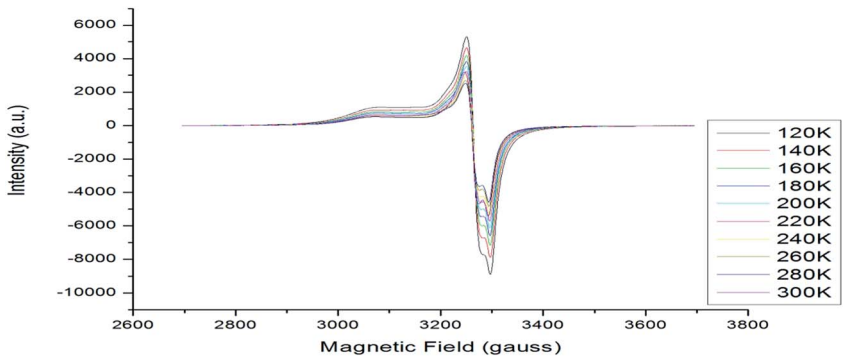

Fig. 15 X-band EPR spectrum of complex **3**.

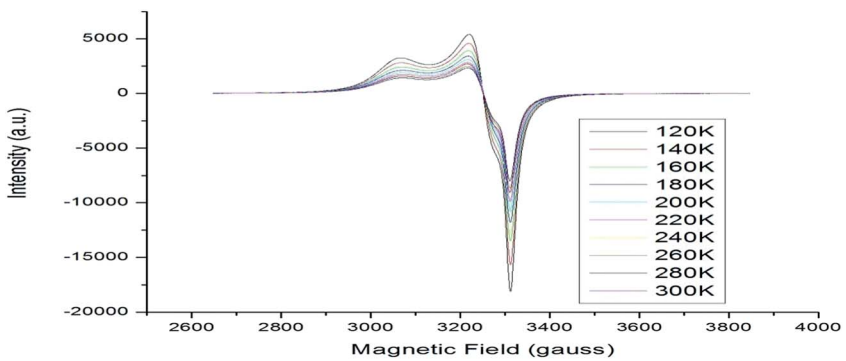

Fig. 16 X-band EPR spectrum of complex **4**.

70% of viable cells were killed in 8 hours of incubation. Complex **10** was inactive while complex **9** killed this bacteria slowly and complete killing occurred in 24 hours. Complexes **1** and **2** also took longer time of 14–24 hours of incubation for complete killing. All complexes were highly effective against *C. albicans* (Fungi) and the maximum taken for complete killing was only 2–4 hours of incubation.

Fig. 22–24 are plots of time taken by a complex to completely kill a microorganism. The complexes plotted along *X*-axis are C1, C2, C7–C10, the same complexes used to study time kill assay. From Fig. 22, it can seen that complex **7** takes only 2 hours to completely kill MRSA, while complex **9** takes 6 hours to completely *S. aureus*. Complexes **7** and **8** have taken 2 hours for completely kill *K. pneumoniae* and *C. albicans* (Fig. 23 and 24) while for *P. aeruginosa* complexes **7** and **8** have taken 6 hours of complete killing. For *Sh. flexneri*, complexes **9** and **10** have taken 8 hours for complete killing (Fig. 22–24).

Cellular toxicity testing using MTT assay

The 3-[(4,5-dimethylthiazol-2-yl)-2,5-diphenyl] tetrazolium bromide (MTT) cytotoxicity assay is measured calorimetrically.[97] It is based on the capacity of mitochondrial succinate dehydrogenase enzymes in living cells (sheep blood used) to reduce the yellow water soluble substrate MTT into an insoluble purple colored

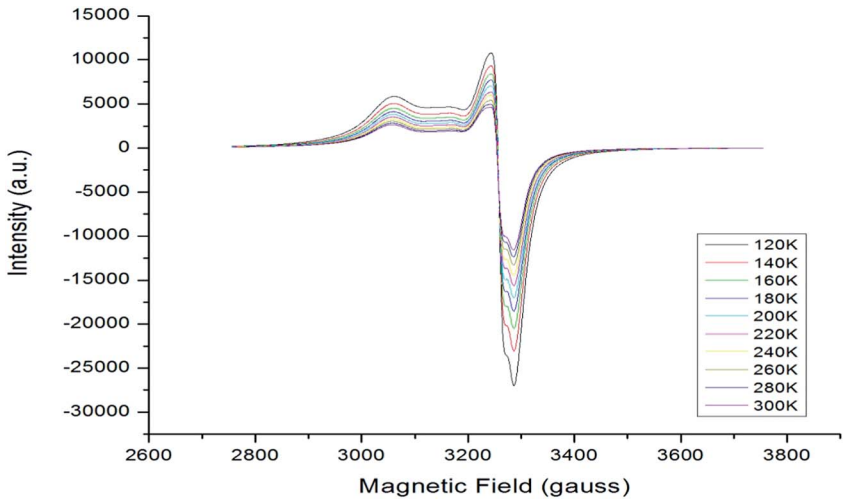

Fig. 17 X-band EPR spectrum of complex **5**.

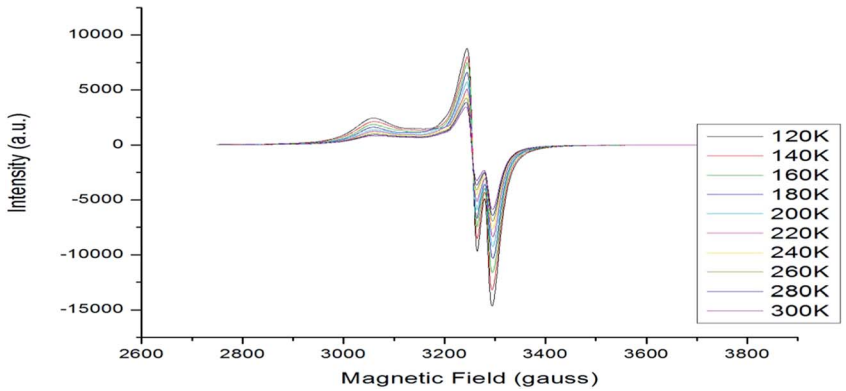

Fig. 18 X-band EPR spectrum of complex **8**.

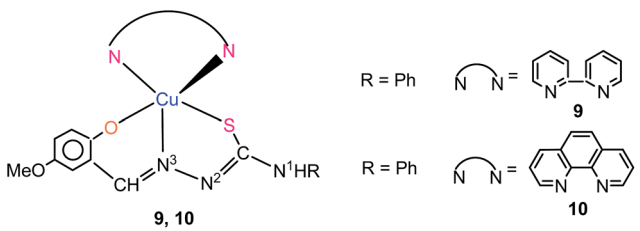

Scheme 5 Copper(II) complexes previously reported.[30]

formazan product which is measured spectrophotometrically. Since, reduction of 3-[(4,5-dimethylthiazol-2-yl)-2,5-diphenyl] tetrazolium bromide (MTT) can only occur in metabolically active cells, where MTT is converted to insoluble formazan crystals that are dissolved in DMSO and the absorbance of purple colored solutions directly represents the viability of the cells. Fig. 25 shows the cytotoxicity levels of complexes **7–10** and about 70–80% of the viable cells were observed. The percentage toxicity was found to be 20–30% in complexes. Among the complexes tested, complex **9** appears to be least followed by complexes **8** and **10** while complex **7** is relatively somewhat more toxic.

It may be pertinent to comment about antimicrobial activity of complexes of thiosemicarbazones with other metals (Ni,[42b,79–82] Pd,[42c,83–87] Pt,[86,87] Zn,[42b,88,89] Cd,[87] Co,[42b], Bi,[89] Sb[90]) against various Gram positive and negative bacteria (*e.g. Bacillus subtilis*, *Staphylococcus aureus*, *Escherichia coli*, *Pseudomonas aeruginosa*, *Penicillium citrinum*, *Saccharomyces cerevisiae*, *Klebsiella pneumoniae*, *methicillin resistant Staphylococcus aureus*) and fungi (*Candida albicans*, *Aspergillus niger*, *Candida guilliermondii*, *Candida parapsilosis*, *Cryptococcus neoformans*). Here thiosemicarbazones used for complexation mostly refer to thioligands other than based on salicylaldehyde moiety at C^2 carbon ($R^1R^2C^2 = N^3–N^2(H)–C(S)–NR^3R^4$). It has been found that the metal complexes exhibit better antimicrobial activity over pure thiosemicarbazones, revealing the role of metals in the antimicrobial activity.[42,79–90] The complexes used in the antimicrobial studies vary in coordination number, nature of the thioligand and the counter anions. The thiosemicarbazones coordinate to the metal in monodentate, bidentate and tridentate fashions. The activity of a complex against a bacteria or fungi varies with the metal and the coordination number. It is further added that cytotoxic activity towards living cells in general is not reported. This makes very difficult to make quantitative

Table 4 Biological data for complexes **1–8**[abc]

Complex[m]/ligand	R	MRSA[f]	*S. aureus*[g]	*K. pneumoniae* 1[h]	*S. flexneri*[i]	*P. aeruginosa*[j]	*C. albicans*[k]
$[Cu(L^1)(bipy)]$**1**	H	20	19	22	18	18	24
$[Cu(L^2)(bipy)]$**3**	Me	20	20	21	19	19	26
$[Cu(L^3)(bipy)]$**5**	Et	24	25	25	21	20	31
$[Cu(L^4)(bipy)]$**7**	Ph	27	25	30	20	22	33
$[Cu(L^1)(phen)]$**2**	H	22	20	20	19	18	25
$[Cu(L^2)(phen)]$**4**	Me	21	20	21	22	19	24
$[Cu(L^3)(phen)]$**6**	Et	24	23	23	20	24	30
$[Cu(L^4)(phen)]$**8**	Ph	28	26	28	20	20	35
$[CuL^1]_n$[l]	H	14	15	16	14	16	14
$[CuL^2]_n$[l]	Me	18	12	16	15	17	17
$[CuL^3]_n$[l]	Et	17	10	16	16	16	18
$[CuL^4]_n$[l]	Ph	18	16	17	16	17	19
H_2L^1	H	13	14	15	—	—	13
H_2L^2	Me	11	12	13	—	10	12
H_2L^3	Et	14	10	13	10	—	14
H_2L^4	Ph	15	15	15	11	—	15
Gentamycin[d/l]							
Amphotericin[e/l]		N.A.	25[d]	32[d]	20[d]	17[d]	34[e]

[a] All measurements are in mm diameter of the inhibition zone (N.A. indicates no activity). [b] The standard deviation varied in the range 0–1 based on three readings. [c] Studies were made in dmso. [d] Commercially available anti-microbial agents. [e] Commercially available anti-microbial agents. [f] Methiciilin resistant *Staphylococcus aureus*. [g] *Staphylococcus aureus*. [h] *Klebsiella pneumoniae* 1. [i] *Shigella flexneri*. [j] *Pseudomonas aeruginosa*. [k] *Candida albicans*. [l] Gentamicin acts as positive control against bacteria (*S. aureus*, *K. pneumoniae* 1, *S. flexneri*, *P. aeruginosa*) and amphotericin acts as positive control against yeast (*Candida albicans*). [m] In complexes **1–8**, the ligands L^{1-4} are O,N,S donors dianions.

Table 5 Minimum inhibitory concentration (MIC in μg mL^{-1}) of copper(II) complexes **1–8**

Complex	MRSA	*S. aureus*	*K. pneumoniae*1	*S. flexneri*	*P. aeruginosa*	*C. albicans*
$[Cu(L^1)(bipy)]$**1**	250	750	250	750	750	50
$[Cu(L^1)(phen)]$**2**	750	750	250	750	750	25
$[Cu(L^2)(bipy)]$**3**	750	750	250	750	750	25
$[Cu(L^2)(phen)]$**4**	250	750	750	250	750	50
$[Cu(L^3)(bipy)]$**5**	50	50	50	250	250	5
$[Cu(L^3)(phen)]$**6**	50	50	50	250	50	10
$[Cu(L^4)(bipy)]$**7**	10	50	10	250	50	5
$[Cu(L^4)(phen)]$**8**	10	50	10	750	750	5

comparison of activity of complexes with one another in view of limited antimicrobial studies. Our investigations involve more systematic approach in the choice of thio-ligand and metal and we have attempted to investigate antimicrobial and cytotoxic activities in more conclusive manner.

Experimental section

General materials and physical methods

Copper(II) acetate monohydrate $Cu(OAc)_2 \cdot H_2O$, thiosemicarbazide, *N*-methyl thiosemicarbazide, *N*-ethyl thiosemicarbazide, *N*-phenyl thiosemicarbazide, 5-nitrosalicylaldehyde, 2,2-bipyridine (bipy) and 1,10-phenanthroline (phen) were procured from Aldrich Sigma Ltd. Elemental analysis C, H, and N were carried out with a thermoelectron FLASHEA1112 analyzer. The melting points were determined with a Gallenkamp electrically heated apparatus. The IR spectra of compounds were recorded in 4000–450 cm^{-1} region with a Perkin Elmer FT-IR Spectrometer by making their KBr pellets. The UV-visible spectra of compounds (10^{-3}–10^{-4} M) were recorded in dimethyl sulfoxide (dmso) with the help of a UV-1601 PC Shimadzu spectrophotometer. Fluorescence spectra of complexes (10^{-4} M) were recorded with a Varian Cary Eclipse Fluorescence spectrophotometer. The ESI-mass spectra were recorded in dmso using Bruker Daltonik LS-MS high resolution microTOF-Q II 10356.

Syntheses. The thio-ligands (L^{1-}, HL^2, HL^3, HL^4, Chart 2) were synthesized according to reported procedures (see ESI†).[91,92]

General method for the synthesis of complexes 1–8

4[Cu(κ³-O,N,S–L¹)(κ²-*N*,*N*-bipy)]·3CH₃OH (1). To a pale yellow solution of thio-ligand H_2 L^1 (0.029 g, 0.127 mmol) in methanol (15 mL) was added dark green solid $Cu(OAc)_2 \cdot H_2O$ (0.025 g, 0.125 mmol) which led to the formation of light brown compound whose analytical data supported the formation of a $[Cu^{II}(O,N,S–L^1]$ (anal. calcd for $C_8H_6CuN_4O_3S$: C 31.84; H 2.00; N 18.57; found: C 31.52; H 1.77; N 19.28%). To a suspension of

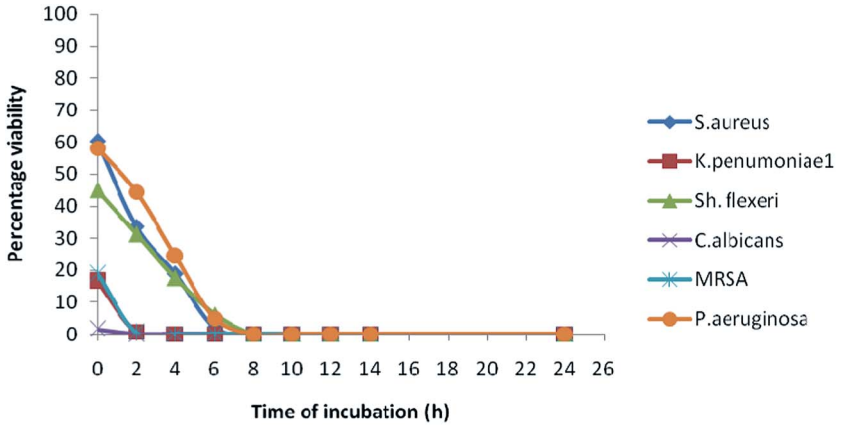

Cu(L^4)(bipy) **7**

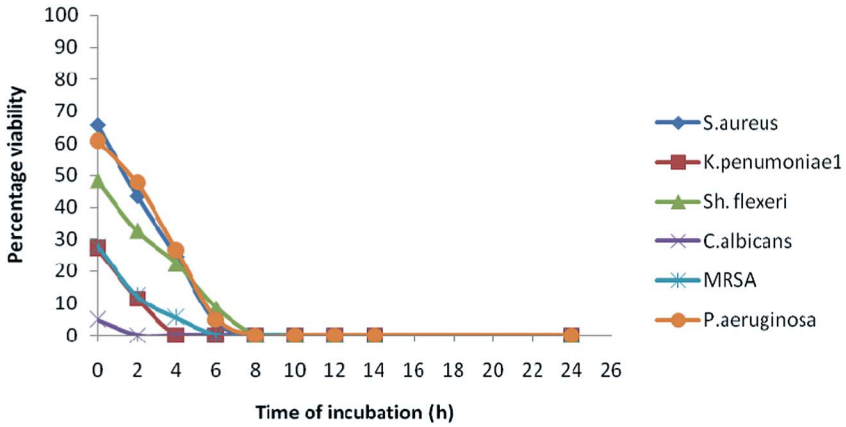

Cu(L^4)(phen) **8**

Fig. 19 Time kill graphs of complexes **7** and **8**. (With phenyl(Ph) substitution at N^1 nitrogen of thio-ligand.

[Cu^{II}(O,N,S–L^1] (0.028 g, 0.092 mmol) in a mixture of dichloromethane and methanol (3 : 1 v/v) was added solid bipy co-ligand (0.014 g, 0.092 mmol) and the contents were stirred for 15 min until a clear dark green solution was formed. The dark green solution was allowed to evaporate at room temperature which yielded a dark green complex. The crystals were grown over a period of 10 days in dichloromethane–methanol mixture (3 : 1 v/v). Dark green crystals (yield 0.031 g, 73%), mp 204 °C. Elemental analysis calculated (%) for $C_{18}H_{14}CuN_6O_3S{\cdot}0.5CH_3OH$: C 46.30; H 3.24; N 18.00; S 7.00; found: C 45.90; H 3.34; N 17.96; S 6.72%. IR (KBr): ν(N^1–H) 3408s; ν(O–H)$_{MeOH}$, 3376s, ν(C–H) 3066s, 2950m; ν(C=N) + ν(C=C) + δ(N–H) 1635s, 1592s, ν(N=O) 1545s, δ(C–H) 1489s, 1471s, 1440s; 1374m, 1349m, δ(N=O) 1312s, ν(C–S) 831s; 805s, 784s, 759s, 726s, 651s, 625s, 516 m, 467s cm^{-1}. UV/vis (DMSO) λ_{max}/nm, ε/L mol^{-1} cm^{-1}: [10^{-3} M] 580m,br (2.14 × 10^2); [10^{-4} M] 392s,br (2.44 × 10^4), 332s,br (2.14 × 10^4), 284m (2.91 × 10^4). Fluorescence spectrum: (λ^{ex}_{max} = 320 nm; λ^{em}_{max} = 429 nm). ESI mass data: calcd for, $C_{18}H_{15}CuN_6O_3S$, [Cu(κ^3-O,N,S–L^1)(κ^2-*N*,*N*-bipy) + H]$^+$ 458.02; obsd *m*/*z* = 458.03. Complexes **2–8** were prepared by a similar method.

Cu(κ^3-O,N,S–L^1)(κ^2-*N*,*N*-phen)] (2). Dark green compound (yield 0.032 g, 75%), mp 241 °C. Elemental analysis calculated (%) for $C_{20}H_{14}CuN_6O_3S$: C 49.84; H 2.93; N 17.44; S 6.65; found: C 48.99; H 2.74; N 17.21; S 6.41%. IR (KBr): ν(N^1–H) 3431br; ν(C–H) 3055w, 2967w, 2922w, ν(C=N) + ν(C=C) + δ(N–H) 1595s, ν(N=O) 1548s, δ(C–H) 1493s, 1426s; 1373s, δ(N=O) 1311s, 1244s, 1100s, 949s, ν(C–S) 837s; 806s, 726s, 653s cm^{-1}. UV/vis (DMSO) λ_{max}/nm, ε/L mol^{-1} cm^{-1}: [10^{-3} M] 592m,br (2.08 × 10^2); [10^{-4} M] 396s,br (2.19 × 10^4), 331br (1.82 × 10^4), 271 m (5.00 × 10^4). Fluorescence spectrum: (λ^{em}_{max} = 426 nm; λ^{ex}_{max} = 320 nm). ESI mass data: calcd for $C_{20}H_{15}CuN_6O_3S$, [Cu(κ^3-O,N,S–L^1)(κ^2-*N*,*N*-phen) + H]$^+$ 482.02; obsd *m*/*z* = 482.02.

[Cu(κ^3-O,N,S–L^2)(κ^2-*N*,*N*-bipy)] (3). Dark green crystals (yield 0.034 g, 78%), mp 207 °C. Elemental analysis calculated (%) for $C_{19}H_{16}CuN_6O_3S$: C 48.35; H 3.42; N 17.81; S 6.79; found: C 48.07; H 3.61; N 17.95; S 6.52%. IR (KBr, selected absorption bands): ν(N^1–H) 3359s; ν(C–H) 3068w, 2931w, 2889m; ν(C=N) + ν(C=C) + δ(N–H) 1601s; ν(N=O) 1547m, 1508 m, δ(C–H) 1474s, 1434s, 1404s, 1371s; δ(N=O) 1312s; 1272s, 1243s, 1193s, 1171s, 1157s, 1070s, 1033s, 1006s, 954s, 898s; ν(C–S) 831s; 763s, 735s, 650s, 623s, 513m, 499w, 484w cm^{-1}. UV/vis (DMSO) λ_{max}/nm,

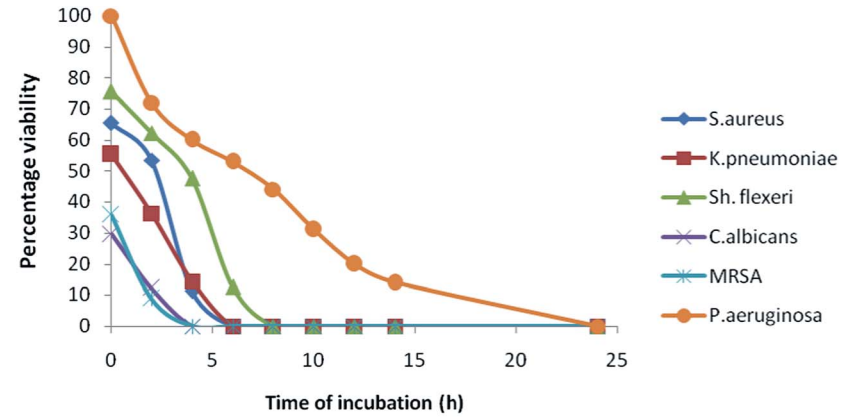

Cu(L)(bipy) **9**

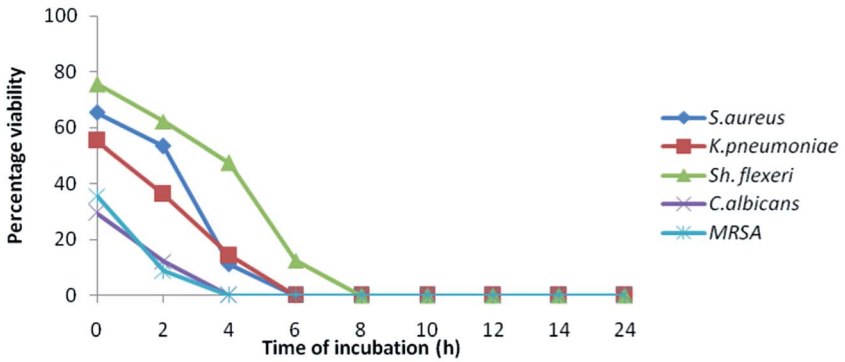

Cu(L)(phen) **10**

Fig. 20 Time kill graph of complexes **9** and **10** reported earlier.[30] (with methoxy substitution at 2-hydroxyohenyl ring and phenyl (Ph) substitution at N^1 nitrogen of thio-ligand).

ε/L mol^{-1} cm^{-1}: [10^{-3} M] 580s,br (1.83 × 10^2); [10^{-4} M] 396s,br (1.82 × 10^4), 329br (1.50 × 10^4), 293 m (1.81 × 10^4). Fluorescence spectrum: (λ^{em}_{max} = 428 nm; λ^{ex}_{max} = 320 nm). ESI mass data: calcd for $C_{19}H_{17}CuN_6O_3S$, [Cu(κ^3-O,N,S–L^2)(κ^2-*N*,*N*-bipy) + H]$^+$ 472.03; obsd *m*/*z* = 472.03.

[Cu(κ^3-O,N,S–L^2)(κ^2-*N*,*N*-phen)] (4). Dark green crystals (yield 0.037 g, 74%), mp 225 °C. Elemental analysis calculated (%) for $C_{21}H_{16}CuN_6O_3S$: C 50.85; H 3.24; N 16.98; S 6.46; found: C 49.93; H 3.37; N 16.72; S 6.29%. IR (KBr): ν(N^1–H) 3361s; ν(C–H) 3059w, 2966w, 2925w, 2867w; ν(C=N) + ν(C=C) + δ(N–H) 1668m, 1597s, ν(N=O) 1547m, 1512m; δ(C–H) 1492s, 1469s, 1428s; 1371w; δ(N=O) 1312s; 1242m, 1298s, 1219s, 1192w, 1146w, 1101s, 954m, 865m,; ν(C–S) 836s; 772w, 727s, 695m, 652m, 625s, 516w, 486w, 466w cm^{-1}. UV/vis (DMSO) λ_{max}/nm, ε/L mol^{-1} cm^{-1}: [10^{-3} M] 594s,br (1.55 × 10^2); [10^{-4} M] 389m,br (1.63 × 10^4), 334br (1.35 × 10^4), 285 m (2.54 × 10^4). Fluorescence spectrum: (λ^{em}_{max} = 425 nm; λ^{ex}_{max} = 320 nm). ESI mass data: calcd for $C_{21}H_{17}CuN_6O_3S$, [Cu(κ^3-O,N,S–L^2)(κ^2-*N*,*N*-phen) + H]$^+$ 495; obsd *m*/*z* = 496.3s.

[Cu(κ^3-O,N,S–L^3) (κ^2-*N*,*N*-bipy) (5). Dark green crystals (yield 0.030 g, 73%), mp 185 °C. Elemental analysis calculated (%) for $C_{20}H_{18}CuN_6O_3S$: C 49.73; H 3.73; N 17.29, S 6.60; found: C 50.28; H 3.65; N 16.96, S 6.63%. IR (KBr): ν(N^1–H) 3365br; ν(C–H) 3074w, 2967w, 2928w, 2854w; ν(C=N) + ν(C=C) + δ(N–H) 1602s, 1561m; ν(N=O) 1549m; 1509w, δ(C–H) 1474s, 1433s, 1398w; 1371m; δ(N=O) 1314s; 1243w, 1135m, 1104s, 1033s, 1024w, 954m, 927w; ν(C–S) 828s; 763s, 731s, 695w, 650m, 611w, 500w, 466w cm^{-1}. UV/vis (DMSO) λ_{max}/nm, ε/L mol^{-1} cm^{-1}: [10^{-3} M] 598s,br (2.26 × 10^2); [10^{-4} M] 403br (2.56 × 10^4), 325s (2.09 × 10^4), 286s (2.64 × 10^4). Fluorescence spectrum: (λ^{em}_{max} = 430 nm; λ^{ex}_{max} = 355 nm). ESI mass data: calcd for $C_{20}H_{19}CuN_6O_3S$, [Cu(κ^3-O,N,S–L^3) (κ^2-*N*,*N*-bipy) + H]$^+$ 486.03; obsd *m*/*z* = 486.03s.

[Cu(κ^3-O,N,S–L^3)(κ^2-*N*,*N*-phen)] (6). Dark green crystals (yield 0.033 g, 79%), mp 197 °C. Elemental analysis calculated (%) for $C_{21}H_{18}CuN_6O_3S$: C 50.65; H 3.64; N 16.87; S 6.44; found: C 50.12; H 3.73; N 16.54; S 6.31%. IR (KBr): ν(N^1–H) 3362br; ν(C–H) 3059m, 2966m, 2924m, 2867m; ν(C=N) + ν(C=C) + δ(N–H) 1597s; ν(N=O) 1547s; 1512s, δ(C–H) 1493s, 1469s, 1428s; δ(N=O) 1311s, 1242s, 1146s, 1101s, 1078s, 954s, 847s; ν(C–S) 834s; 757s, 727s, 695s, 655s, 640s, 516m, 486m, 466m cm^{-1}. UV/vis (DMSO) λ_{max}/nm, ε/L mol^{-1} cm^{-1}: [10^{-3} M] 584br (2.18 × 10^2); [10^{-4} M] 397s,br (2.27 × 10^4), 331s (1.89 × 10^4), 291m (4.55 × 10^4). Fluorescence spectrum: (λ^{em}_{max} = 434 nm; λ^{ex}_{max} = 355 nm). ESI mass data: calcd for, [Cu(κ^3-O,N,S–L^3) (κ^2-*N*,*N*-phen) + H]$^+$ $C_{21}H_{19}$-CuN_6O_3S, 510.05; obsd *m*/*z* = 510.05.

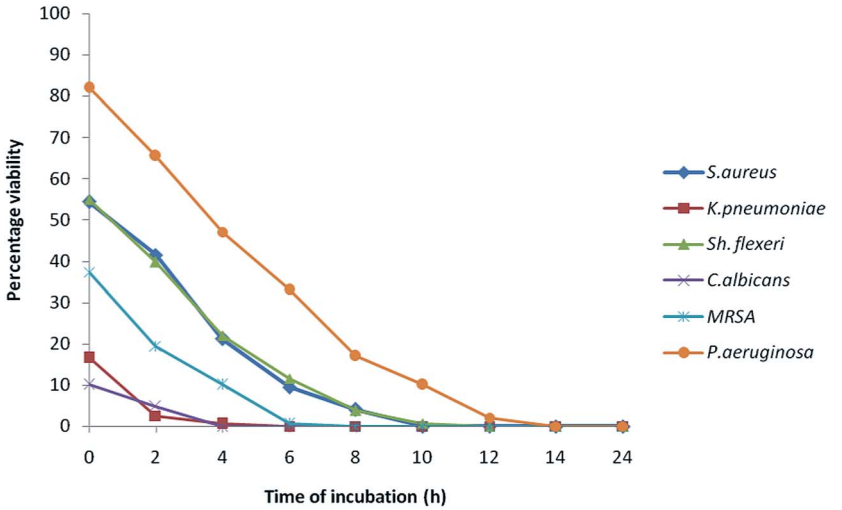

$Cu(L^1\text{-}NH_2)(bipy)$ **1**

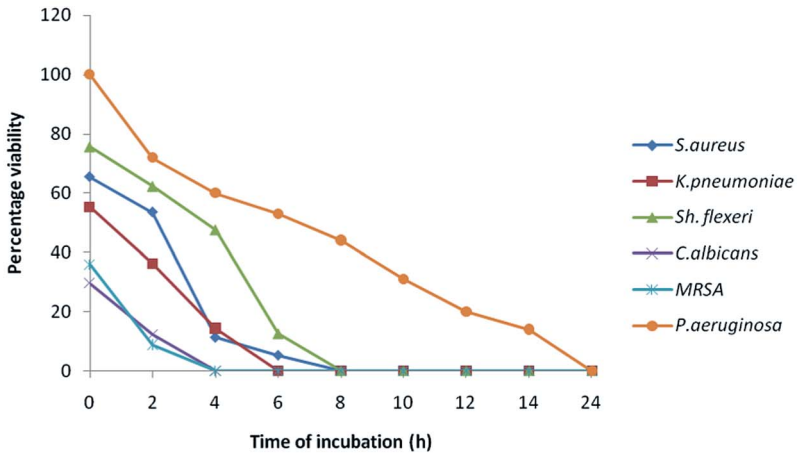

$Cu(L^1\text{-}NH_2)(phen)$ **2**

Fig. 21 Time kill graph of complexes **1** and **2**. (With Hydrogen(H) substitution at N^1 nitrogen of thio-ligand.

[Cu(κ³-O,N,S–L⁴)(κ²-*N*,*N*-bipy)] (7). Dark green crystals (yield 0.034 g, 85%), mp 227 °C. Elemental analysis calculated (%) for $C_{24}H_{18}CuN_6O_3S$: C 53.98; H 3.40; N 15.74; S 6.00; found: C 54.12; H 3.63; N 16.03; S 5.95%. IR (KBr): $\nu(N^1\text{–}H)$ 3374s, ν(C–H) 3069br, 3043m, 2924br; ν(C═N) + ν(C═C) + δ(N–H) 1596s; ν(N═O) 1547s; 1538s; δ(C–H) 1496s, 1432s; 1371m, 1340m, δ(N═O) 1317s; 1245m, 1184s, 1136m, 1184m, 1103s, 1070s, 955m, 895m; ν(C–S) 828s; 769s, 746s, 734m, 688m, 653m, 615m, 465m cm^{-1}. UV/vis (DMSO) λ_{max}/nm, ε/L mol^{-1} cm^{-1}: [10^{-3} M] 590br (2.8×10^2); [10^{-4} M] 406s,br (2.69×10^3), 332s (2.63×10^4), 294m (2.25×10^4), 266m (3.95×10^4). Fluorescence spectrum: ($\lambda^{em}_{max} = 433$ nm; $\lambda^{ex}_{max} = 320$ nm). ESI mass data: calcd for $C_{24}H_{19}CuN_6O_3S$, [Cu(κ³-O,N,S–L^4) (κ²-*N*,*N*-bipy) + H]$^+$ 534.03; obsd $m/z = 534.04$s.

[Cu(κ³-O,N,S–L⁴)(κ²-*N*,*N*-phen)] (8). Dark green crystals (yield 0.031 g, 76%), mp 239 °C. Elemental analysis calculated (%) for $C_{26}H_{18}CuN_6O_3S$: C 55.96; H 3.25; N 15.06; S 5.75; found: C 56.15; H 3.36; N 15.18; S 5.58%. IR (KBr): $\nu(N^1\text{–}H)$ 3364s; ν(C–H) 3165m, 2924br, 2853m; ν(C═N) + ν(C═C) + δ(N–H 1599s, ν(N═O) 1548s, δ(C–H)1498s, 1469m, 1432s; 1374m, δ(N═O) 1314s, 1244s, 1185m, 1132m, 1100s, 956s, 896m; ν(C–S) 829s, 749s, 726s, 691m, 658m, 641m, 585m, 558m, 516m, 504m, 464m cm^{-1}. Electronic absorption spectrum ($10^{-3}/10^{-4}$ m in dmso, λ_{max}/nm, ε/L mol^{-1} cm^{-1}: [10^{-3} M] 585br (1.85×10^2), [10^{-3} M] 420m,br (1.23×10^4), 343s (1.61×10^4), 328s (2.10×10^4), 282m (3.91×10^4). Fluorescence spectrum: ($\lambda^{em}_{max} = 426$ nm; $\lambda^{ex} = 320$ nm). ESI mass data: calcd for $C_{26}H_{19}CuN_6O_3S$, [Cu(κ³-O,N,S–L^4) (κ²-*N*,*N*-phen) + H]$^+$ 558.05; obsd $m/z = 558.05$s.

X-ray crystallography

A single crystal was mounted on a glass fiber and used for data collection with a Xcalibur, Eos, Gemini (**3**, **6**), and a Bruker Kapa – Apex (II) CCD diffractometer (**1**, **4**, **5**, **7**, **8**), equipped with graphite monochromated Mo-Kα ($\lambda = 0.71073$ Å). Crystal data

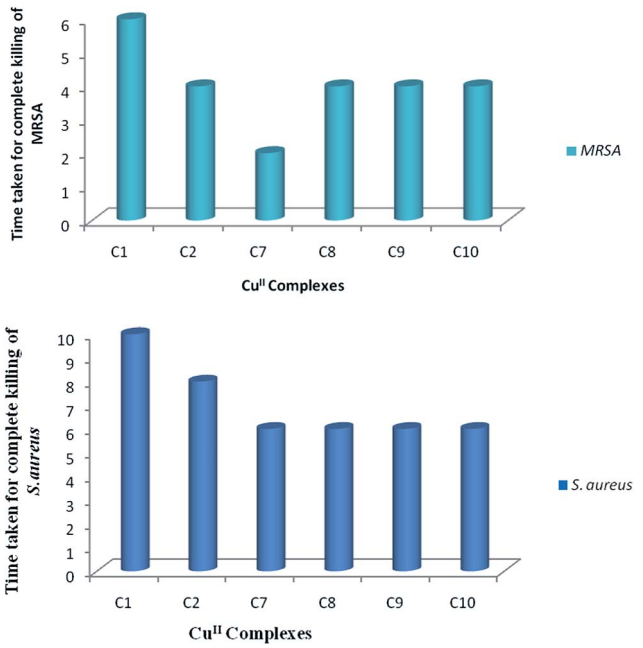

Fig. 22 Time taken for complete killing of MRSA and *S. aureus*.

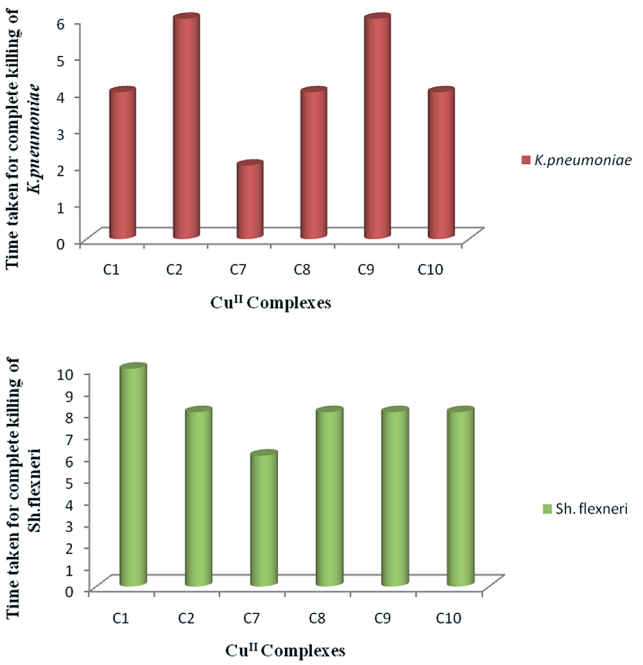

Fig. 23 Time taken for complete killing of *K. pneumoniae* and *Sh. flexneri*.

were collected at 173 (2) (**4**, **6**), 296 (2) (**1**, **3**, **5**, **7**, **8**) K. For complexes **3** and **6** data were processed with CrysAlisPro CCD (data collection), CrysAlisPro RED (cell refinement, data reduction).[93] The structures were solved by direct methods using the program Olex2 1.2, refined by full-matrix least-squares techniques against F^2 using SHELX-97 and molecular graphics from Olex 2.[94] For complexes **1**, **3**, **5** and **7** data were processed with Bruker Kapa – Apex(II) CCD and corrected for absorption

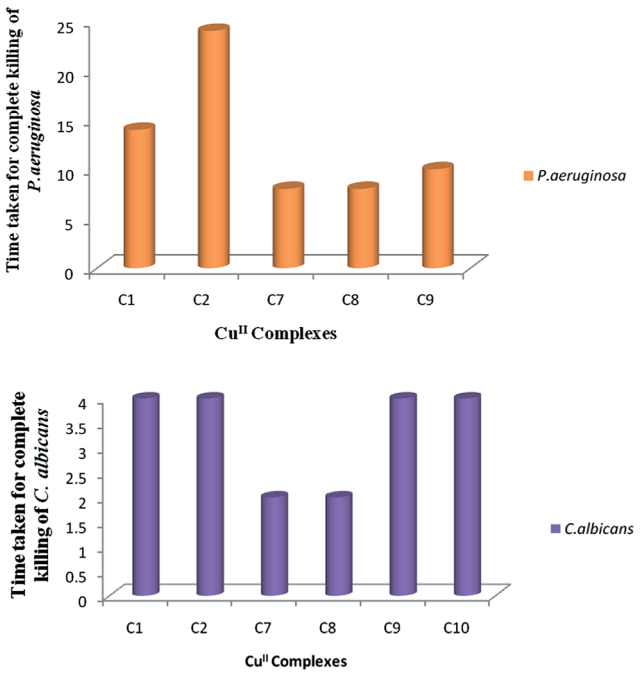

Fig. 24 Time taken for complete killing of *P. aeruginosa* and *C. albicans*.

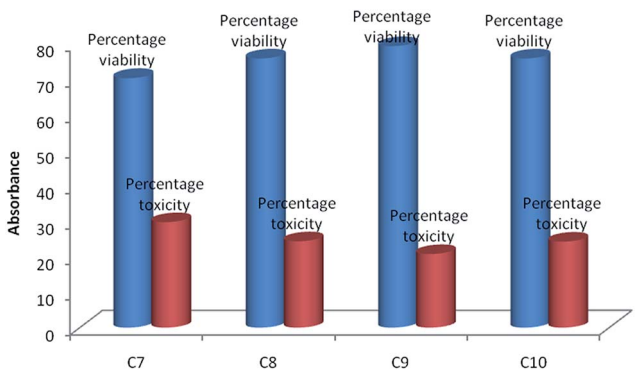

Fig. 25 Cytotoxicity levels of complexes studied.

using SADABS.[95] The structures were solved by direct methods using SIR-92 software[95] and refined by full-matrix least-squares method based on F^2 using the program SHELX-97.[94] All non-hydrogen atoms were refined anisotropically.

Antimicrobial studies

Test organisms. The reference strains of bacteria and yeasts were obtained from Microbial Type Culture Collection (MTCC), Institute of Microbial Technology (IMTECH), Chandigarh, India and the clinical isolate methicillin resistant *Staphylococcus aureus* (MRSA) was obtained from Post graduate Institute of Medical Education and Research, (PGIMER), Chandigarh, India. Reference strains included Gram positive bacteria: *Staphylococcus aureus* (MTCC-740), Gram negative bacteria: *Klebsiella pneumoniae* (MTCC-109), *Pseudomonas aeruginosa*

(MTCC-741), *Shigella flexneri* (MTCC-1457) and one yeast strain: *Candida albicans* (MTCC-227).

Inoculum preparation. A loopful of isolated bacterial and yeast colonies were inoculated into 5 ml of their respective medium and incubated at 37 °C and 25 °C respectively for 4 h. This was used as inoculum after adjusting the turbidity as per Mc Farland turbidity standard. This turbidity is equivalent to approximately 1 to 2 × 10^8 colony forming units per ml (CFU ml^{-1}). The inoculum thus prepared was used further for further testing.

Minimum inhibitory concentration (MIC). Minimum inhibitory concentration of the selected compounds was worked out by agar dilution method.[96] A stock solution of (5 mg mL^{-1}) concentration was prepared and incorporated into Muller Hinton agar medium for bacteria and yeast malt extract medium for yeast. The final concentrations of the compound in the medium containing plates ranged from (0.005–3 mg mL^{-1}). These plates were then inoculated with 0.1 mL of the activated bacterial and yeast strains by streaking with a sterile tooth pick. The plates were incubated at 37 °C for bacteria and 25 °C for yeast for 24 h. The lowest concentration of the extract causing complete inhibition of the microbial growth was taken as MIC. The results were compared with that of control in which the sample was replaced with DMSO.

Time kill assay. The time kill assay for the selected purified compounds was performed by viable cell count method (VCC).[96] A stock solution of (1 mg mL^{-1}) was prepared. Five ml of 4 h grown inoculum was adjusted to 0.5 McFarland standard and serially diluted to 10^{-3} with respective double strength broth medium. Equal volume of each diluted inoculum and the extract to be tested were mixed at their respective predetermined MIC values and incubated at respective temperature of 25 °C for yeast and 37 °C for bacteria. At different time intervals *viz.* 0, 1, 2, 3, 4… 24 h, 0.1 mL of the mixed suspension was spread on suitable agar plates in duplicate and incubated for 24 h at suitable temperature. The mean number of colonies were determined and compared with that of control, in which the compounds were replaced with DMSO.

Cellular toxicity testing using MTT assay. The cellular toxicity of the compounds was determined by MTT (3-[(4,5-dimethylthiazol-2-yl)-2,5-diphenyl] tetrazolium bromide) assay.[97] Ten millilitre sheep blood was taken into injection syringe containing 3 mL Alsever's solution (anticoagulant) and transferred to sterile centrifuge tubes. The blood was centrifuged at 1600×*g* at room temperature (25 ± 3 °C) for 20 min to separate the plasma from the cells. The supernatant was discarded and 6 mL phosphate buffer saline (PBS) added which was again centrifuged. The RBCs were washed thrice with PBS by centrifugation and the pellet was resuspended in 6 mL of PBS. Various dilutions of these cells using PBS were prepared and counted with the help of a haemocytometer under a light microscope so as to obtain cells equivalent to 1 × 10^5 CFU mL^{-1}. The following formula was used to determine the required number of cells: Number of cells per mL = Number of cells counted in 25 squares × Dilution factor × 10^4. The cell suspension thus prepared was dispensed into Elisa plates (100 μL per well) and incubated at 37 °C for overnight. The supernatant was removed carefully and 200 μL of the extract and the purified compound was added and incubated further for 24 h. Supernatant was removed again and added 20 μL MTT solutions (5 mg mL^{-1}) to each well and incubated further for 3 h at 37 °C on orbital shaker at 60 rpm. After incubation, the supernatant was removed without disturbing the cells and 50 μL DMSO was added to each well to dissolve the formazan crystals. The absorbance was measured at 590 nm using an automated microplate reader (Biorad 680-XR, Japan). The wells with untreated cells served as control.

Conclusion

In the present study, copper(II) complexes (**1–8**) of salicylaldehyde-N substituted thiosemicarbazones having 5-nitro-substitution in the 2-hydroxy phenyl ring along with different substituents at N^1 nitrogen using 2,2′-bipyridine and 1,10-phenanthroline as co-ligands have shown significant growth inhibitory activity against *Staphylococcus aureus* (MTCC740), methicillin resistant *Staphylococcus aureus* (MRSA), *Klebsiella pneumoniae* 1 (MTCC109), *Shigella flexneri* (MTCC1457), *Pseudomonas aeruginosa* (MTCC741) and *Candida albicans* (MTCC227). It is interested to note that complexes **1–8** are highly active against *Shigella flexneri* (MTCC1457) and *Pseudomonas aeruginosa* (MTCC741) while only few complexes with 5-methoxy substitution at 2-hydroxyphenyl ring of thio-ligand are active against these microorganisms. Also, the results are encouraging especially related to MRSA since the activity against MRSA is an interesting observation as the commercially available gentamycin is found to be inactive against this bacterial strain. From time kill studies it has also been found that all the complexes were found to be bactericidal in nature and complex **7** followed by complex **8** with phenyl substitution at N^1 nitrogen of thio-ligand took lesser time for complete killing of microorganisms in comparison of complexes **9** and **10** with 5-methoxy-substitution in the 2-hydroxy phenyl ring and phenyl substitution at N^1 nitrogen of thio-ligand except only in case for *Sh. flexeneri*. The cytotoxicity levels of complexes **7–10** through MTT assay reveals that about 70–80% of the normal cells are viable. The percentage toxicity was found to be very low and complex **9** appears to be least toxic followed by complexes **8** and **10** while complex **7** is relatively somewhat more toxic.

Acknowledgements

Financial assistance from the University Grant Commission (BSR, UGC); the Council of Scientific and Industrial Research (CSIR), New Delhi; Emeritus Grant [21(0904)/12-EMR-II] to TSL; and the Department of Science and Technology (DST) ST for the X-ray diffractometer grant to the department are gratefully acknowledged. Authors thank Dr Alfonso Castineiras and Dr Isabel Garcia Santo (University of Santiago, Spain) for providing x-band (9.4 GHz) EPR spectra.

References

1 B. A. Gingras, R. W. Hornal and C. H. Bayley, *Can. J. Chem.*, 1960, **38**, 712–720.

2 M. A. Ali and S. E. Livingstone, *Coord. Chem. Rev.*, 1974, **13**, 101–132.
3 M. J. M. Campbell, *Coord. Chem. Rev.*, 1975, **15**, 279–319.
4 S. Padhye and G. B. Kauffman, *Coord. Chem. Rev.*, 1985, **63**, 127–160.
5 D. X. West, S. Padhye and P. B. Sonawane, *Struct. Bonding*, 1991, 1–50.
6 D. X. West, A. E. Liberta, S. Padhye, R. C. Chilkate, P. B. Sonawane, A. S. Kumbhar and R. G. Yerande, *Coord. Chem. Rev.*, 1993, **123**, 49–71.
7 J. S. Casas, M. S. Garcia-Tasende and J. Sordo, *Coord. Chem. Rev.*, 1999, **193**, 283–359.
8 J. S. Casas, M. S. Garcia-Tasende and J. Sordo, *Coord. Chem. Rev.*, 2000, **209**, 197–261.
9 T. S. Lobana, R. Sharma, G. Bawa and S. Khanna, *Coord. Chem. Rev.*, 2009, **253**, 977–1055.
10 T. S. Lobana, G. Bawa, A. Castineiras, R. J. Butcher and M. Zeller, *Organometallics*, 2008, **27**, 175–180.
11 T. S. Lobana, G. Bawa, G. Hundal and M. Zeller, *Z. Anorg. Allg. Chem.*, 2008, **634**, 931–937.
12 J. Martinez, M. T. Pereira, I. Buceta, G. Alberdi, A. Amoedo, J. J. Fernandez, M. Lopez-Torres and J. M. Vila, *Organometallics*, 2003, **22**, 5581–5584.
13 J. Dutta, S. Datta, D. K. Seth and S. Bhattacharya, *RSC Adv.*, 2012, 11751–11763.
14 J. Dutta and S. Bhattacharya, *RSC Adv.*, 2013, 10707–10721.
15 S. Datta, D. K. Seth, R. J. Butcher and S. Bhattacharya, *Inorg. Chim. Acta*, 2011, **377**, 120–128.
16 R. K. Mahajan, T. P. S. Walia, Sumanjit and T. S. Lobana, *Anal. Sci.*, 2006, **22**, 389–392.
17 R. K. Mahajan, I. Kaur and T. S. Lobana, *Talanta*, 2003, **59**, 101–105.
18 R. K. Mahajan, T. P. S. Walia, Sumanjit and T. S. Lobana, *Talanta*, 2005, **67**, 755–759.
19 H. R. Fatondji, S. Kpoviessi, F. Gbaguidi, J. Bero, V. Hannaert, J. Quetin-Leclercq, J. Poupaert, M. Moudachirou and G. C. Accrombessi, *Med. Chem. Res.*, 2013, **22**, 2151–2162.
20 T. S. Lobana, P. Kumari, A. Castineiras and R. J. Butcher, *Eur. J. Inorg. Chem.*, 2013, 3557–3566.
21 T. S. Lobana, P. Kumari, A. Castineiras, R. J. Butcher, T. Akitsu and Y. Aritake, *Dalton Trans.*, 2011, **40**, 3219–3228.
22 T. S. Lobana, P. Kumari, R. J. Butcher, T. Akitsu, Y. Aritake, F. Fernandez, J. Perles and M. C. Vega, *J. Organomet. Chem.*, 2012, **701**, 17–26.
23 T. S. Lobana, R. Sharma and R. J. Butcher, *Polyhedron*, 2009, **28**, 1103–1110.
24 T. S. Lobana, G. Bawa and R. J. Butcher, *Inorg. Chem.*, 2008, **47**, 1488–1495.
25 T. S. Lobana, S. Indoria, M. Sharma, J. Nandi, J. A. Jassal, M. S. Hundal and A. Castineiras, *Polyhedron*, 2014, **80**, 34–40.
26 T. S. Lobana, P. Kumari, R. J. Butcher, J. P. Jasinski and J. A. Golen, *Z. Anorg. Allg. Chem.*, 2012, **638**, 1861–1867.
27 T. S. Lobana, S. Khanna, R. Sharma, G. Hundal, R. Sultana, M. Chaudhary, R. J. Butcher and A. Castineira, *Cryst. Growth Des.*, 2008, **8**, 1203–1212.
28 T. S. Lobana, S. Khanna and R. J. Butcher, *Inorg. Chem. Commun.*, 2008, **11**, 1433–1435.
29 T. S. Lobana, Rekha, R. J. Butcher, T. W. Failes and P. Turne, *J. Coord. Chem.*, 2005, **58**, 1369–1375.
30 T. S. Lobana, S. Indoria, A. K. Jassal, H. Kaur, D. S. Arora and J. P. Jasinski, *Eur. J. Med. Chem.*, 2014, **76**, 145–154.
31 P. D. Bonnitcha, A. L. Vajvere, J. S. Lewis and J. R. Dilworth, *J. Med. Chem.*, 2008, **51**, 2985–2991.
32 P. Wolohan, Y. Jeongsoo, J. W. Michael and E. R. David, *J. Med. Chem.*, 2005, **48**, 5561–5569.
33 J. R. Dilworth and R. Hueting, *Inorg. Chim. Acta*, 2012, **389**, 3–15.
34 R. L. Arrowsmith, P. A. Waghorn, M. W. Jones, A. Bauman, S. K. Brayshaw, Z. Hu, G. Kociok-Kohn and T. L. Mindt, *Dalton Trans.*, 2011, **40**, 6238–6252.
35 S. I. Pascu, P. A. Waghorn, B. W. C. Kennedy, R. Arrowsmith, S. R. Bayly, J. R. Dilworth, M. Christlie, R. M. Tyrrell, J. Zhong, R. M. Kowalczyk, D. Collison, P. K. Aley, G. C. Churchill and F. I. Aigbirhio, *Chem.–Asian J.*, 2010, **5**, 506–519.
36 S. I. Pascu, P. A. Waghorn, T. D. Conry, B. Lin, H. M. Betts, J. R. Dilworth, R. B. Sim, G. C. Churchill, F. I. Aigbirhio and J. E. Warren, *Dalton Trans.*, 2008, 2107–2110.
37 S. I. Pascu, P. A. Waghorn, T. D. Conry, H. M. Betts, J. R. Dilworth, G. C. Churchill, T. Pokrovska, M. Christlieb, F. I. Aigbirhio and J. E. Warren, *Dalton Trans.*, 2007, 4988–4997.
38 M. Christlieb, A. R. Cowley, J. R. Dilworth, P. S. Donnelly, B. M. Paterson, H. S. R. Struthers and J. M. White, *Dalton Trans.*, 2007, 327–331.
39 R. I. Maurer, P. J. Blower, J. R. Dilworth, C. A. Reynolds, Y. Zheng and G. E. D. Mullen, *J. Med. Chem.*, 2002, **45**, 1420–1431.
40 M. Christlieb and J. R. Dilworth, *Chem.–Eur. J.*, 2006, **12**, 6194–6206.
41 K. A. Price, A. Caragounis, B. M. Paterson, G. Filiz, I. Volitakis, C. L. Masters, K. J. Barnham, P. S. Donnelly, P. J. Crouch and A. R. White, *J. Med. Chem.*, 2009, **52**, 6606–6620.
42 (*a*) M. C. Rodriguez-Argu, E. C. Lopez-Silva, J. Sanmartin, P. Pelagatti and F. Zani, *J. Inorg. Biochem.*, 2005, **99**, 2231–2239; (*b*) M. C. Rodríguez-Argüelles, P. Tourón-Touceda, R. Cao, A. M. García-Deibe, P. Pelagatti, C. Pelizzi and F. Zani, *J. Inorg. Biochem.*, 2009, **103**, 35–42; (*c*) T. Rosu, E. Pahontu, S. Pasculescu, R. Georgescu, N. Stanica, A. Curaj, A. Popescu and M. Leabu, *Eur. J. Med. Chem.*, 2010, **45**, 1627–1634.
43 I. C. Mendes, J. P. Moreira, A. S. Mangrich, S. P. Balena, B. L. Rodrigues and H. Beraldo, *Polyhedron*, 2007, **26**, 3263–3270.
44 T. Rosu, A. Gulea, A. Nicolae and R. Georgescu, *Molecules*, 2007, **12**, 782–796.
45 (*a*) I. Babahan, F. Eyduran, E. P. Coban, N. Orhan, D. Kazar and H. Biyik, *Spectrochim. Acta, Part A*, 2014, **121**, 205–215; (*b*) A. Bacchi, M. Carcelli, P. Pelagatti, C. Pelizzi, G. Pelizzi and F. Zani, *J. Inorg. Biochem.*, 1999, **75**, 123–133.

46 K. O. Ferraza, S. M. S. V. Wardell, J. L. Wardell, S. R. W. Louroc and H. Beraldoa, *Spectrochim. Acta, Part A*, 2009, **73**, 140–145.

47 A. G. Majouga, M. I. Zvereva, M. P. Rubtsova, D. A. Skvortsov, A. V. Mironov, D. M. Azhibek, O. O. Krasnovskaya, V. M. Gerasimov, A. V. Udina, N. I. Vorozhtsov, E. K. Beloglazkina, L. Agron, L. V. Mikhina, A. V. Tretyakova, N. V. Zyk, N. S. Zefirov, A. V. Kabanov and O. A. Dontsova, *J. Med. Chem.*, 2014, **57**, 6252–6258.

48 P. J. Jansson, P. C. Sharpe, P. V. Bernhardt and D. R. Richardson, *J. Med. Chem.*, 2010, **53**, 5759–5769.

49 W. E. Antholine, J. M. Knight and D. H. Petering, *J. Med. Chem.*, 1976, **19**, 339–341.

50 Z. Afrasiabi, E. Sinn, P. P. Kulkarni, V. Ambike, S. Padhye, D. Deobagakar, M. Heron, C. Gabbutt, C. E. Anson and A. K. Powell, *Inorg. Chim. Acta*, 2005, **358**, 2023–2030.

51 M. B. Ferrari, S. Capacchi, G. Pelosi, G. Reffo, P. Tarasconi, R. Albertini, S. Pinelli and P. Lunghi, *Inorg. Chim. Acta*, 1999, **286**, 134–141.

52 M. B. Ferrari, F. Bisceglie, G. Pelosi, P. Tarasconi, R. Albertini and S. Pinelli, *J. Inorg. Biochem.*, 2001, **87**, 137–147.

53 B. M. Zeglis, V. Divilov and J. S. Lewis, *J. Med. Chem.*, 2011, **54**, 2391–2398.

54 L. A. Saryan, E. Ankel, C. Krishnamurti and D. H. Petering, *J. Med. Chem.*, 1979, **22**, 1218–1221.

55 E. A. Coats, S. R. Milstein, M. A. Pleiss and J. A. Roesener, *J. Med. Chem.*, 1978, **21**, 804–809.

56 E. A. Britta, A. P. B. Silva, T. Ueda-Nakamura, B. P. Dias-Filho, C. C. Silva, R. L. Sernaglia and C. V. Nakamura, *PLoS One*, 2012, **7**(8), 1–12.

57 B. G. Patil, B. R. Havinale, J. M. Shallom and M. P. Chitnis, *J. Inorg. Biochem.*, 1989, **36**, 107–113.

58 A. M. Thomas, A. D. Naik, M. Nethaji and A. R. Chakravarty, *Inorg. Chim. Acta*, 2004, **357**, 2315–2323.

59 V. I. Prisakar, V. I. Tsapkov, S. A. Buracheeva, M. S. Byrke and A. P. Gulya, *J. Pharm. Chem.*, 2005, **39**, 30–32.

60 P. Bindu, M. R. P. Kurup and T. R. Satyakeerty, *Polyhedron*, 1999, **18**, 321–331.

61 R. P. John, A. Sreekanth, V. Rajakannan, T. A. Ajith and M. R. P. Kurup, *Polyhedron*, 2004, **23**, 2549–2559.

62 D. X. West, Y. Yang, T. L. Klein, K. I. Goldberg, A. E. Liberta, J. V. Martinez and R. A. Toscano, *Polyhedron*, 1995, **141**, 1681–1693.

63 D. X. West, M. M. Salberg, G. A. Bain and A. E. Liberta, *Transition Met. Chem.*, 1997, **22**, 180–184.

64 A. D. Naik, P. A. N. Reddy, M. Nethaji and A. R. Chakravarty, *Inorg. Chim. Acta*, 2003, **349**, 149–159.

65 A. B. Lever, *Inorganic electronic spectroscopy*, Elsevier, New York, 2nd edn, 1984, vol. 636.

66 M. Kurosu, P. N. K. Biswas, R. Dhiman and D. C. Crick, *J. Med. Chem.*, 2007, **50**, 3973–3975.

67 Y. Hirokawa, H. Kinoshita, T. Tanaka, K. Nakata, N. Kitadai, K. Fujimoto, S. Kashimoto, T. Kojima and S. Kato, *J. Med. Chem.*, 2008, **51**, 1991–1994.

68 S. Bera, G. G. Zhanel and F. Schweizer, *J. Med. Chem.*, 2008, **51**, 6160–6164.

69 E. J. Begg and M. L. Barclay, *Br. J. Clin. Pharmacol.*, 1995, **39**, 597–603.

70 M. P. Mingeot-Leclercq, Y. Glupczynski and P. M. Tulkens, *Antimicrob. Agents Chemother.*, 1999, **43**, 727–737.

71 M. P. Mingeot-Leclercq and P. M. Tulkens, *Antimicrob. Agents Chemother.*, 1999, **43**, 1003–1012.

72 J. Starr, M. F. Brown, L. Aschenbrenner, N. Caspers, Y. Che, B. S. Gerstenberger, M. Huband, J. D. Knafels, M. M. Lemmon, C. Li, S. P. McCurdy, E. McElroy, M. R. Rauckhorst, A. P. Tomaras, J. A. Young, R. P. Zaniewski, V. Shanmugasundaram and S. Han, *J. Med. Chem.*, 2014, **57**, 3845–3855.

73 R. Silvestri, M. Artico, G. J. Regina, A. D. Pasquali, G. D. Martino, F. D. D'Auria, L. Nencioni and A. T. Palamara, *J. Med. Chem.*, 2004, **47**, 3924–3926.

74 F. Manetti, D. Castagnolo, F. Raffi, A. T. Zizzari, S. Rajamaki, S. D'Arezzo, P. Visca, A. Cona, M. E. Fracasso, D. Doria, B. Posteraro, M. Sanguinetti, G. Fadda and M. Botta, *J. Med. Chem.*, 2009, **52**, 7376–7379.

75 A. Trabocchi, C. Mannino, F. Machetti, F. D. Bernardis, S. Arancia, R. Cauda, A. Cassone and A. Guarna, *J. Med. Chem.*, 2010, **53**, 2502–2509.

76 M. P. Pereira and S. O. Kelley, *J. Am. Chem. Soc.*, 2011, **133**, 3260–3263.

77 M. N. Alekshun and S. B. Levy, *Cell*, 2007, **128**, 1037–1050.

78 S. Mandal, N. K. Pal, I. H. Chowdhury and M. Debmandal, *Pol. J. Microbiol.*, 2009, **58**, 57–60.

79 N. C. Kasuga, K. Sekino, C. Koumo, N. Shimada, M. Ishikawa and K. Nomiya, *J. Inorg. Biochem.*, 2001, **84**, 55–65.

80 N. C. Kasuga, Y. Hara, C. Koumo, K. Sekino and K. Nomiya, *Acta Crystallogr., Sect. C: Cryst. Struct. Commun.*, 1999, **55**, 1264–1267.

81 H. B. Shawish, M. J. Paydar, C. Y. Looi, Y. L. Wong, E. Movahed, S. N. A. Halim, W. F. Wong, M.-R. Mustafa and M. J. Maah, *Transition Met. Chem.*, 2014, **39**, 81–94.

82 M. A. Ali, A. H. Mirza, R. J. Butcher, M. T. H. Tarafder and M. A. Ali, *Inorg. Chim. Acta*, 2001, **320**, 1–6.

83 R. Prabhakaran, S. V. Renukadevi, R. Karvembu, R. Huang, J. Mautz, G. Huttner, R. Subashkumar and K. Natarajan, *Eur. J. Med. Chem.*, 2008, **43**, 268–273.

84 D. Kovala-Demertzi, M. A. Demertzis, E. Filiou, A. A. Pantazaki, P. N. Yadav, J. R. Miller, Y. Zheng and D. A. Kyriakidis, *BioMetals*, 2003, **16**, 411–418.

85 P. Kalaivani, R. Prabhakaran, E. Ramachandran, F. Dallemer, G. Paramaguru, R. Renganathan, P. Poornima, V. V. Padma and K. Natarajan, *Dalton Trans.*, 2012, **41**, 2486–2499.

86 N. C. Kasuga, A. Ohashi, C. Koumo, J. Uesugi, M. Oda and K. Nomiya, *Chem. Lett.*, 1997, 609–610.

87 K. Alomar, A. Landreau, M. Kempf, M. A. Khan, M. Allain and G. Bouet, *J. Inorg. Biochem.*, 2010, **104**, 397–404.

88 N. C. Kasuga, K. Sekino, M. Ishikawa, A. Honda, M. Yokoyama, S. Nakano, N. Shimada, C. Koumo and K. Nomiya, *J. Inorg. Biochem.*, 2003, **96**, 298–310.

89 K. Nomiya, K. Sekino, M. Ishikawa, A. Honda, M. Yokoyama, N. C. Kasuga, H. Yokoyama, S. Nakano and K. Onodera, *J. Inorg. Biochem.*, 2004, **98**, 601–615.

90 N. C. Kasuga, K. Onodera, S. Nakano, K. Hayashi and K. Nomiya, *J. Inorg. Biochem.*, 2006, **100**, 1176–1186.
91 T. S. Lobana, P. Kumari, G. Hundal and R. J. Butcher, *Polyhedron*, 2010, **29**, 1130–1136.
92 T. S. Lobana, A. Sanchez, J. S. Casas, A. Castineiras, J. Sordo, M. S. G. Tasende and E. M. V. Lopez, *J. Chem. Soc., Dalton Trans.*, 1997, 4289–4299.
93 Oxford Diffraction, *CrysAlisPro CCD and CrysAlisPro RED*, Oxford Diffraction Ltd., Yarnton, England, 2009.
94 O. V. Dolomanov, L. J. Bourhis, R. J. Gildea, J. A. K. Howard and H. Puschmann, *J. Appl. Crystallogr.*, 2009, **42**, 339–341.
95 A. Altomare, G. Cascarano, C. Giacovazzo and A. Guagliardi, *J. Appl. Crystallogr.*, 1993, **26**, 343–350.
96 G. J. Kaur and D. S. Arora, *BMC Complementary Altern. Med.*, 2009, **09**, 30.
97 G. Ciapetti, E. Cenni, L. Pratelli and A. Pizzoferrato, *Biomaterials*, 1993, **14**, 359–364.